Uekita Takamasa Jia Lin Narisawa-Saito Mako Yokota Jun Kiyono Tohru Sakai Ryuichi	CUB domain-containing protein 1 is a novel regulator of anoikis resistance in lung adenocarcinoma.	Mol.Cel. Biol.	27 (21)	7649-7660	2007
Tazaki Tatsuya Miyazaki Kazuo Hiyama Eiso Nakamoto Tetsuya Sakai Ryuichi Yamasaki Norimasa Honda Zen-ichiro Noda Masaki Miyasaka Nobuyuki Sueda Taijiro Honda Hiroaki	Functional analysis of Src homology 3-encoding exon (exon 2) of p130Cas in primary fibroblasts derived from exon 2-specific knockout mice.	Genes Cells	13 (2)	145-157	2008
Jia Lin Uekita Takamasa Sakai Ryuichi	Hyperphosphorylated cortactin in cancer cells plays an inhibitory role in cell motility by regulating tyrosine phosphorylation of p130Cas.	*Mol. Cancer. Res.*	in press		2008
Uekita Takamasa Tanaka Masamitsu Takigahara Misato Miyazawa Yuri Nakanishi Yukihiro Kanai Yae Yanagihara Kazuyoshi Sakai Ryuichi	CUB-domain containing protein 1 (CDCP1) regulates peritoneal dissemination of gastric scirrhous carcinoma	Am. J. Pathol.	in press		2008
Futamura M, Kamino H, Miyamoto Y, Kitamura N, Nakamura Y, Ohnishi S, Masuda Y and Arakawa H	Possible role of Semaphorin 3F, a candidate tumor suppressor gene at 3p21.3, in p53-regulated tumor angiogenesis suppression	Cancer Research	67 (4)	1451-1460	2007
Bourdon A, Minai L, Serre V, Jais JP, Sarzi E, Aubert S, Chretien D, de Lonlay P, Paquis-Flucklinger V, Arakawa H, Nakamura Y, Munnich A and Rotig A	Mutation of RRM2B, encoding p53-controlled ribonucleotide reductase (p53R2), causes severe mitochondrial DNA depletion	Nature Genetics	39 (6)	776-780	2007
Kazuji Ohmori, Yoshie Endo, Yusuke Yoshida, Hirokazu Ohata, Yoichi Taya and Masato Enari	Monomeric but not trimeric clathrin heavy chain regulates p53-mediated transcription.	Oncogene	27	2215-2227	2008

Yoshie Endo, Atsumi Sugiyama, Shun-Ai Li, Kazuji Ohmori, Hirokazu Ohata, Yusuke Yoshida, Masabumi Shibuya, Kohji Takei, Masato Enari and Yoichi Taya	Regulation of Clathrin-Mediated Endocytosis by p53.	Genes to Cells	13	375-386	2008

Vol 446|5 April 2007|doi:10.1038/nature05673

LETTERS

Foxp3 controls regulatory T-cell function by interacting with AML1/Runx1

Masahiro Ono[1,2]*, Hiroko Yaguchi[3]*, Naganari Ohkura[3]*, Issay Kitabayashi[4], Yuko Nagamura[3], Takashi Nomura[1], Yoshiki Miyachi[2], Toshihiko Tsukada[3] & Shimon Sakaguchi[1,5]

Naturally arising $CD25^+CD4^+$ regulatory T cells (T_R cells) are engaged in the maintenance of immunological self-tolerance and immune homeostasis by suppressing aberrant or excessive immune responses, such as autoimmune disease and allergy[1–3]. T_R cells specifically express the transcription factor Foxp3, a key regulator of T_R-cell development and function. Ectopic expression of Foxp3 in conventional T cells is indeed sufficient to confer suppressive activity, repress the production of cytokines such as interleukin-2 (IL-2) and interferon-gamma (IFN-γ), and upregulate T_R-cell-associated molecules such as CD25, cytotoxic T-lymphocyte-associated antigen-4, and glucocorticoid-induced TNF-receptor-family-related protein[4–7]. However, the method by which Foxp3 controls these molecular events has yet to be explained. Here we show that the transcription factor AML1 (acute myeloid leukaemia 1)/Runx1 (Runt-related transcription factor 1), which is crucially required for normal haematopoiesis including thymic T-cell development[8–11], activates *IL-2* and *IFN-γ* gene expression in conventional $CD4^+$ T cells through binding to their respective promoters. In natural T_R cells, Foxp3 interacts physically with AML1. Several lines of evidence support a model in which the interaction suppresses IL-2 and IFN-γ production, upregulates T_R-cell-associated molecules, and exerts suppressive activity. This transcriptional control of T_R-cell function by an interaction between Foxp3 and AML1 can be exploited to control physiological and pathological T-cell-mediated immune responses.

Functional studies of the *IL-2* promoter have ascertained that a minimal promoter region extending to 300 base pairs (bp) relative to the transcription start site of the *IL-2* gene, containing binding sites for nuclear factor of activated T cells (NFAT), Oct1, activator protein-1 (AP-1) and nuclear factor-κB (NF-κB)[12], is sufficient for inducible expression of the gene after stimulation of the T-cell antigen receptor (TCR) in reporter assays[13]. However, the upstream sequences beyond this region also enhance promoter activity[12]. By examining the 2.0-kb 5′ flanking region of the mouse *IL-2* gene, we have found three putative AML1–DNA binding consensus sites (5′-ACCACA-3′) at −370, −1,327 and −1,458 bp (relative to the transcription start site), denoted RE1, RE2 and RE3, respectively (Fig. 1a). In particular, a region containing the proximal RE1 site is highly conserved between humans, mice and other mammalian species (Supplementary Fig. S1) and is reported to be selectively and rapidly demethylated on T-cell activation[14].

To determine whether AML1 binds to the *IL-2* promoter and modifies *IL-2* gene expression, we performed several assays with mouse primary $CD4^+$ T cells and human Jurkat cells. In chromatin immunoprecipitation (ChIP) assays using an antibody against AML1, the *IL-2* promoter region adjacent to the RE1 site was co-precipitated in mouse primary $CD4^+$ T cells, whereas the 5′ and 3′ regions far from the start site were not (Fig. 1b). The human *IL-2* promoter region encompassing the AML1 site corresponding to the mouse RE1 site was also co-precipitated with the anti-AML1 antibody in Jurkat cells (Fig. 1b). Electrophoretic mobility-shift assays showed specific retardation of the complexes formed between the DNA-binding domain of AML1 and radiolabelled oligonucleotides corresponding to RE1, RE2 and RE3 (Fig. 1c). Moreover, mutating the RE1, RE2 and RE3 sites by altering two nucleotides at each site (mut RE1, mut RE2 and mut RE3; Supplementary Fig. S2) completely abolished AML1 binding (Fig. 1c).

To examine the functional responsiveness of the *IL-2* promoter to AML1, we made a reporter construct composed of the 1.6-kb *IL-2* promoter, containing the three AML1-binding sites, fused to a luciferase reporter gene. Stimulation of Jurkat cells with anti-CD3 and anti-CD28 activated the *IL-2* promoter in the construct[15], and transfection of AML1 enhanced this activation further (Fig. 1d). The use of a mutated *IL-2* promoter with mut RE1, mut RE2 and mut RE3 sites (*IL-2* promoter ΔAML-*luc*) resulted in a striking decrease in both stimulation-induced and AML1-enhanced promoter activities (Fig. 1e). Mutations that disrupted NFAT sites (*IL-2* promoter ΔNFAT-*luc*) led to a complete elimination of both stimulation-induced transcription activation and AML1-enhanced transactivation (Fig. 1f), suggesting that AML1-dependent activation of the *IL-2* promoter is reliant on the NFAT transcription factor complex.

Knockdown of endogenous *AML1* by RNA interference (RNAi) in Jurkat cells resulted in a marked decrease in IL-2 production after stimulation, indicating that AML1 is physiologically required for the induction of IL-2 expression in activated T cells (Fig. 1g). Moreover, in mouse primary T cells retrovirally transduced with *AML1*, IL-2 production in response to anti-CD3 and anti-CD28 stimulation was much higher than in empty-vector-transduced T cells (Fig. 1h, i). Conversely, IL-2 production was markedly reduced in mouse T cells transduced with a dominant-negative form of AML1 (AML1-DN, also called AML1a (ref. 16); see Fig. 2d), which lacks the C-terminal transcriptional activation and inhibition domains (Fig. 1h, i).

Taken together, the findings in Fig. 1 indicate that AML1 binds specifically to the AML1 sites present in the *IL-2* promoter region, thus enhancing *IL-2* gene expression.

Expression of AML1 protein in both conventional T cells and T_R cells (Supplementary Fig. S3) and strong repression of IL-2 expression by Foxp3 (Fig. 1h, i, refs 4–6) indicate that AML1 and Foxp3 may interact in T_R cells and may thereby control IL-2 expression. Indeed, an anti-FOXP3 antibody co-precipitated endogenous FOXP3 with AML1 from human peripheral blood mononuclear cells (PBMCs) (Fig. 2a). This indicates *in vivo* physiological interaction of

[1]Department of Experimental Pathology, Institute for Frontier Medical Sciences, and [2]Department of Dermatology, Graduate School of Medicine, Kyoto University, Kyoto 606-8507, Japan. [3]Tumor Endocrinology Project, and [4]Molecular Oncology Division, National Cancer Center Research Institute, Chuo-ku Tokyo, 104-0045, Japan. [5]Core Research for Evolutional Science and Technology (CREST), Japan Science and Technology Agency, Kawaguchi 332-0012, Japan.
*These authors contributed equally to this work.

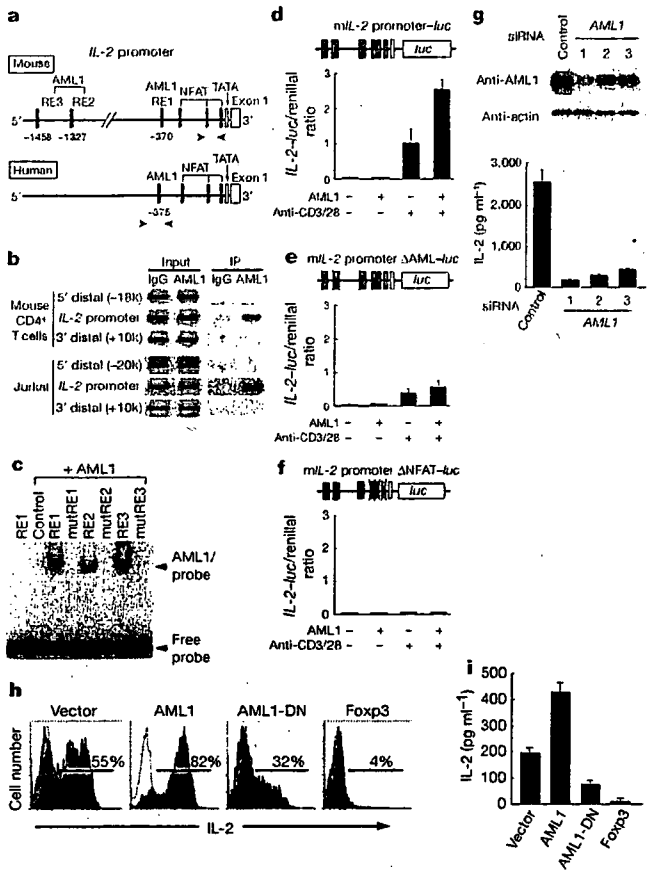

Figure 1 | AML1/Runx1 enhances IL-2 expression through binding to the *IL-2* promoter in activated T cells. **a**, Schematic representation of the mouse and human *IL-2* promoters. The putative AML1 binding sites, the NFAT sites and the TATA boxes are shown in red, blue and yellow, respectively. **b**, In ChIP assays performed with an antibody against AML1 or control rabbit IgG, aliquots of chromatin obtained before (Input) or after immunoprecipitation (IP) from mouse $CD4^+$ T cells or Jurkat cells were analysed by polymerase chain reaction with primers specific for the *IL-2* promoter. The positions of the ChIP primers are delineated in **a** by arrowheads. The primers for the 5′ and 3′ far distal regions were used as controls. **c**, In an electrophoretic mobility-shift assay, the DNA-binding domain of AML1 was incubated with radiolabelled oligonucleotides spanning the individual AML1 wild-type or mutated (mut) RE1, RE2 and RE3 sites on the *IL-2* promoter (sequences of the oligonucleotides are shown in Supplementary Fig. S2). **d–f**, Jurkat cells were simultaneously transfected with either an AML1-expressing or an empty vector, and with wild-type mouse *IL-2* (m*IL-2*) promoter–luciferase (*luc*) (**d**), a mutated promoter ΔAML–*luc* construct containing mut RE1, mut RE2 and mut RE3 (**e**), or a mutated promoter ΔNFAT–*luc* construct containing mutated NFAT consensus sites (**f**). Cells were either unstimulated or stimulated by plate-bound anti-CD3 and soluble anti-CD28 for 6 h, and luciferase activities were measured. Data shown are relative values of firefly luciferase normalized to *Renilla* luciferase and are expressed as means ± s.e.m. **g**, Jurkat cells were transfected with *AML1* siRNAs (1, 2 and 3) or control siRNA, and the expression of endogenous AML1 was evaluated by western blot analysis (top). Cells transfected with the indicated siRNAs were stimulated for 24 h with plate-bound anti-CD3 and soluble anti-CD28, and IL-2 levels in the supernatant were quantified by ELISA (bottom; means ± s.d.). **h**, Mouse $CD25^-CD4^+$ T cells were transduced with retroviral pMCsIg vectors encoding indicated proteins, IRES and GFP. GFP-positive cells were sorted and stimulated by plate-bound anti-CD3 and soluble anti-CD28 for 6 h and analysed for intracellular IL-2 expression by flow cytometry. Thin lines represent control staining with an isotype-matched antibody. **i**, Sorted GFP-positive cells were stimulated by soluble anti-CD3 and anti-CD28 with antigen-presenting cells for 24 h, and IL-2 levels in the supernatant were quantified by ELISA (means ± s.d.). Results represent three independent experiments.

endogenous FOXP3 and AML1 in natural T_R cells, because most $FOXP3^+$ T cells in PBMCs are naturally arising $CD4^+$ T_R cells[17–20]. Glutathione *S*-transferase (GST) pulldown experiments showed physical interaction of these two molecules *in vitro*: [^{35}S]methionine-labelled Foxp3 bound to the GST–AML1 fusion protein but not to the GST protein alone, and, reciprocally, labelled AML1 bound to GST–Foxp3 (Fig. 2b). In addition, under confocal microscopy, immunostained endogenous AML1 and Foxp3 were heterogeneously distributed in the nucleus and partly co-localized in mouse $CD25^+CD4^+$ T_R cells, suggesting that both proteins comprise part of the same molecular complex in natural T_R cells (Fig. 2c).

We next attempted to determine the Foxp3-interacting domain of AML1 and the AML1-interacting domain of Foxp3. In reciprocal co-immunoprecipitation experiments using lysates of human embryonic kidney 293T cells co-transfected with constructs encoding tagged AML1 and Foxp3 proteins, deletion mutants of AML1 lacking

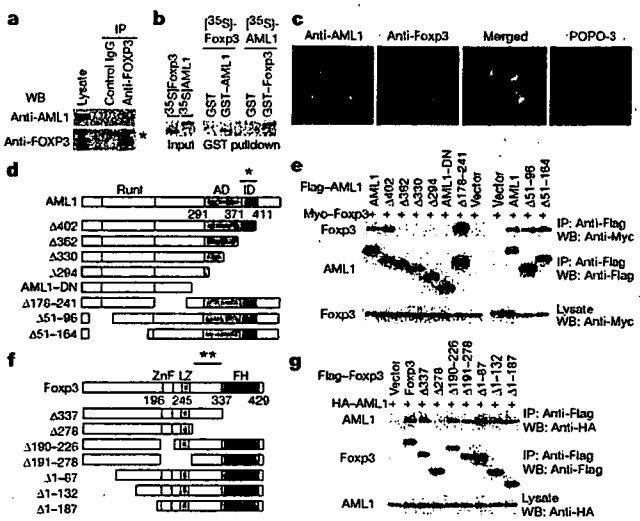

Figure 2 | Foxp3 interacts physically with AML1. **a**, Endogenous interaction between AML1 and FOXP3 in human PBMCs. PBMCs were lysed, subjected to immunoprecipitation (IP) with anti-FOXP3 antibody or control IgG, and western blotted (WB) with anti-AML1 and anti-FOXP3 antibodies. Asterisk indicates immunoglobulin heavy chain. **b**, *In vitro* interaction between Foxp3 and AML1 was analysed by GST pulldown assays. *In vitro* transcribed/translated [^{35}S]methionine-labelled FoxP3 or AML1 was incubated with bacterially expressed GST–AML1 or GST–Foxp3, respectively. GST alone was included as a negative control. Input consisted of 10% of the [^{35}S]methionine-labelled products. **c**, The intracellular localizations of endogenous AML1 and Foxp3 in mouse T_R cells were analysed by confocal microscopy with antibodies directed against AML1 and Foxp3. A representative image of a single T_R cell is shown. Images of AML1 (green) and Foxp3 (red) were merged to show regions of co-localization (yellow). The nucleus was revealed with POPO-3 staining (blue). **d**, Schematic diagram of wild-type AML1 (shown on top) and the deletion constructs. The Runt, activation and inhibition domains are indicated as Runt, AD and ID, respectively. **e**, Myc-tagged Foxp3 was co-transfected into 293T cells with the indicated Flag-tagged AML1 constructs and immunoprecipitated with anti-Flag M2 agarose; protein blots were probed with anti-Myc (top) or anti-Flag (middle) antibodies. The expression of Foxp3 in the lysates was monitored by immunoblotting with an anti-Myc antibody (bottom). **f**, Schematic diagram of wild-type Foxp3 (top) and the deletion constructs. The zinc finger, leucine zipper and forkhead domains are indicated as ZnF, LZ and FH, respectively. **g**, Haemagglutinin (HA)-tagged AML1 was co-transfected into 293T cells with the indicated Flag-tagged Foxp3 constructs and immunoprecipitated with anti-Flag M2 agarose, and protein blots were probed with anti-HA (top) or anti-Flag (middle) antibodies. The expression of AML1 in the lysates was monitored by immunoblotting with an anti-HA antibody (bottom). Figures represent three independent experiments.

the carboxy-terminal region (amino acids 362–402; asterisk in Fig. 2d) failed to bind to Foxp3, indicating a requirement of this region for interaction with Foxp3 (Fig. 2d, e). This region of AML1 corresponds to the domain that was shown to have inhibitory activity on transcription[21]. Similar experiments using deletion mutants of Foxp3 indicated that the AML1-interacting domain of the Foxp3 protein was located between the forkhead domain and the leucine zipper motif (amino acids 278–336; asterisks in Fig. 2f) (Fig. 2f, g).

ChIP assays showed that Foxp3 bound to the *IL-2* promoter (Supplementary Fig. S4), as reported recently[22]. To establish the functional significance of the interaction between Foxp3 and AML1, we used the same *IL-2* reporter construct described in Fig. 1d to examine whether Foxp3 affects the transactivation activity of AML1 in Jurkat cells (Fig. 3a). Foxp3 did indeed repress both stimulation-induced transcriptional activation and AML1-dependent transcriptional enhancement of the *IL-2* promoter. When the mutated *IL-2* promoter ΔAML1-*luc* (depicted in Fig. 1e) was employed, *IL-2* promoter activity was substantially attenuated and Foxp3 failed to repress the transcription further, suggesting that the repression of *IL-2* transcription by Foxp3 is dependent on AML1 (Fig. 3b).

Next, to determine whether Foxp3 is also able to repress AML1-mediated IL-2 production in mouse primary T cells, we co-transduced $CD25^-CD4^+$ conventional T cells with retroviral constructs of Foxp3–internal ribosome entry site (IRES)–nerve growth factor receptor (NGFR) and AML1–IRES–green fluorescent protein (GFP), and analysed IL-2 production in those T cells co-expressing NGFR and GFP (Fig. 3c, d). Consistent with the results of the luciferase reporter assays was our observation that Foxp3 repressed AML1-driven IL-2 production in the co-transduced T cells (Fig. 3c, d, and Supplementary Fig. S5a). In addition, retroviral gene transduction of AML1 failed to elicit IL-2 production in Foxp3-expressing natural $CD25^+CD4^+$ T_R cells (Fig. 3e, and Supplementary Fig. S5b).

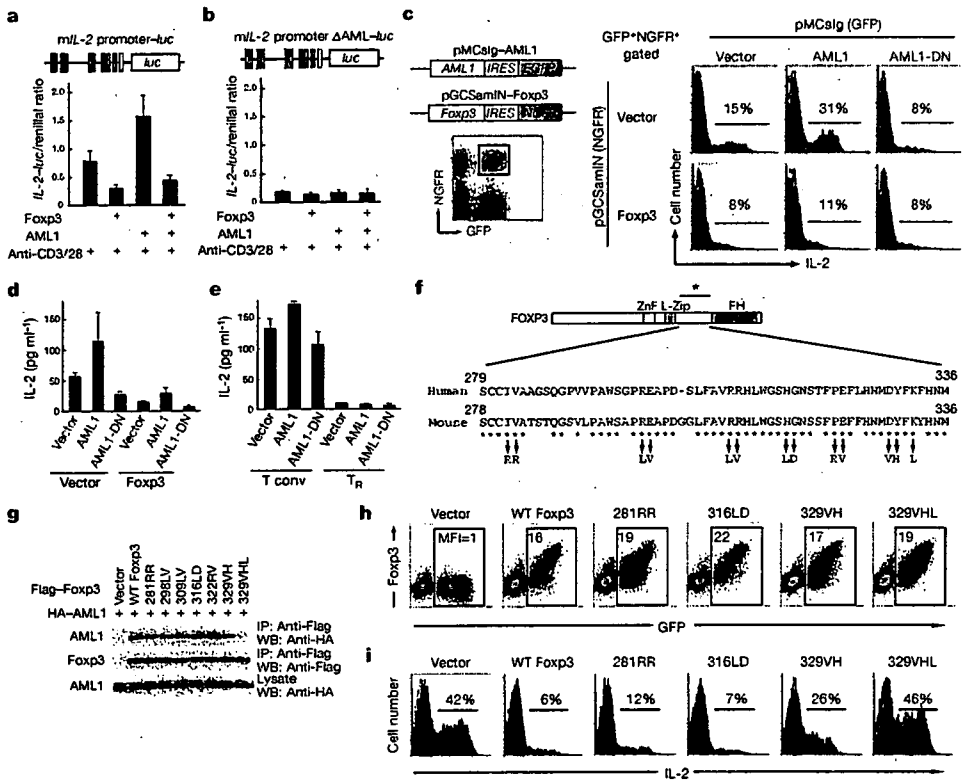

Figure 3 | Foxp3 represses AML1-induced IL-2 expression by interacting with AML1. **a**, **b**, Jurkat cells were co-transfected with expression vectors for the indicated proteins and wild-type *IL-2* promoter (**a**) or mutated *IL-2* promoter ΔAML–*luc* constructs (**b**), stimulated as in Fig. 1d–f, and luciferase activities were measured. **c**, Schematic representation of the retroviral vectors, including pMCsIg–AML1 (*AML1–IRES–GFP*) and pGCSamIN–Foxp3 (*Foxp3–IRES–NGFR*), which were used to express AML1 and Foxp3, respectively, in this study. Mouse $CD4^+$ T cells were co-transduced with the pMCsIg and pGCSamIN vectors to express the indicated proteins and were activated by soluble anti-CD3 and anti-CD28 for 6 h. Cells were stained with a biotinylated anti-NGFR antibody and allophycocyanin-conjugated streptavidin, and subsequently fixed and stained with phycoerythrin-conjugated anti-IL-2, and analysed by flow cytometry for intracellular IL-2 in $GFP^+/NFGR^+$ double-positive cells (rectangles). **d**, Co-transduced mouse $CD4^+$ T cells sorted by gating $GFP^+/NFGR^+$ double-positive cells were stimulated as in Fig. 1i, and IL-2 levels in the supernatant were quantified by ELISA. **e**, Mouse $CD25^-CD4^+$ conventional T cells (T conv) or $CD25^+CD4^+$ T cells (T_R) were transduced with the pMCsIg vectors to express the indicated proteins, sorted by gating GFP^+ cells and stimulated as in Fig. 1i; IL-2 levels in the supernatant were quantified by ELISA. Expression of transduced genes in **d** and **e** was confirmed by western blot analysis with sorted GFP^+NGFR^+ (or GFP^+) cells (Supplementary Fig. S5). **f**, Sequence alignment of the AML1-binding region in human and mouse FOXP3. Substitutions were introduced at conserved residues of human/mouse FOXP3 (asterisks) as indicated. **g**, Haemagglutinin (HA)-tagged AML1 was co-transfected into 293T cells with the indicated Flag-tagged Foxp3 mutants and immunoprecipitated with anti-Flag M2 agarose, and protein blots were probed with anti-HA (top) or anti-Flag (middle) antibodies. The expression of AML1 in the lysates was monitored by immunoblotting using an anti-HA antibody (bottom). WT, wild type. Abbreviations of mutants are as follows: 281RR: I281R and V282R; 298LV: R298L and E299V; 309LV: R309L and R310V; 316LD: H316L and G317D; 322RV: P322R and E323V; 329VH: D329V and Y330H; 329VHL: D329V, Y330H and K332L. **h**, Mouse $CD4^+$ T cells transduced with pMCsIg vectors encoding wild-type and mutant Foxp3 proteins, IRES and GFP were stained intracellularly with phycoerythrin-conjugated anti-Foxp3, and analysed by flow cytometry. Numbers in dot plots indicate mean fluorescence intensity (MFI) of Foxp3 in the rectangle gates. **i**, Gene-transduced T cells were stimulated as in Fig. 1h, and $CD4^+$ cells were analysed for intracellular IL-2 by flow cytometry. Error bars represent s.e.m.; all experiments were repeated at least three times with similar results.

To examine further whether IL-2 repression by Foxp3 is dependent on the interaction of Foxp3 with AML1, we made Foxp3 mutants with two or three amino acid substitutions in the region required for interaction with AML1 (Fig. 3f). In co-immunoprecipitation experiments using these Foxp3 mutants and wild-type AML1, mutant 329VHL, which has three amino acid changes in the region, scarcely bound to AML1, and mutant 329VH exhibited less AML1 binding than other mutants with two amino acid substitutions or than wild-type Foxp3 (Fig. 3g). After retroviral gene transduction of mutated or wild-type Foxp3 into conventional $CD4^+$ T cells, the expression levels of the Foxp3 proteins were equivalent (Fig. 3h). However, the AML1-non-binding 329VHL mutant was unable to suppress IL-2 production when transduced to conventional $CD4^+$ T cells, and the 329VH mutant with reduced AML1 binding was less suppressive than other mutants or wild-type expressers (Fig. 3i). 329VHL is not a simple loss-of-function mutant, because it retained the ability to interact with NFAT (Supplementary Fig. S6) and regulate some Foxp3-regulated genes in a DNA microarray analysis (Supplementary Fig. S7). Thus, in addition to the NFAT–Foxp3 interaction[22], the AML1–Foxp3 interaction is critical on its own for suppressing IL-2.

We next examined whether AML1 is involved in the regulation of the genes encoding T_R-cell-associated cell surface molecules, such as CD25, cytotoxic T-lymphocyte-associated antigen-4 (CTLA-4) and glucocorticoid-induced TNF-receptor-family-related protein (GITR). ChIP assays showed that AML1 bound to intron 1 of *CD25*, to the promoter of *CTLA-4*, and to the promoter and intron 1 of *GITR* (Supplementary Fig. S8a, b). ChIP assays using the same primer pairs as in Fig. S8a showed that Foxp3 bound to *CD25* intron 1 and *GITR* intron 1 (Supplementary Fig. S9), which was consistent with recent reports[22]. Retroviral transduction of AML1 in mouse primary $CD4^+$ T cells downregulated the expression of CD25, CTLA-4 and, in particular, GITR (Supplementary Fig. S8c), whereas similar transduction of wild-type Foxp3 upregulated the expression of these molecules (Fig. 4a). Notably, the 329VHL Foxp3 mutant failed to upregulate them, and the 329VH mutant was less efficient in the upregulation than other mutants or wild-type Foxp3 (Fig. 4a). Taken together, these findings suggest that AML1 and the Foxp3–AML1 complex control these genes in conventional T cells and natural T_R cells, respectively.

We, and others, have shown previously that natural T_R cells and Foxp3-transduced T cells are anergic (that is, non-proliferative) on stimulation of the TCR *in vitro*, whereas stimulation of the TCR together with high-dose IL-2 and anti-CD28 stimulation can abrogate the anergic state[4,5,23,24]. As shown in Fig. 4b, c, 329VHL-transduced T cells were slightly less anergic than T cells transduced with other mutants or wild-type Foxp3, and the addition of high-dose IL-2 and anti-CD28 antibody more easily abrogated their anergic state. Furthermore, whereas natural T_R cells and Foxp3-transduced T cells suppress the proliferation of co-cultured naive T cells on stimulation of the TCR *in vitro*[4,5,23,24], the 329VHL-transduced cells were much less suppressive than T cells transduced with other mutants (Fig. 4d). In addition, knockdown of AML1 in human $CD25^{high}CD4^+$ T cells abrogated their anergic state and attenuated their suppressive activity (Fig. 4e–g, and Supplementary Fig. S10). Taken together, these results support a model in which the formation of the Foxp3–AML1 complex controls anergy and the suppressive function of natural T_R cells.

AML1 and the Foxp3–AML1 complex may control the expression of a broad range of genes in addition to those encoding the IL-2 and T_R-cell-associated molecules described above (Supplementary Fig. S7). For example, AML1 and Foxp3 controlled IFN-γ production in a similar manner to that of IL-2: AML1 activated *IFN-γ* gene transcription by binding to its promoter, and Foxp3 suppressed AML1-induced IFN-γ production (Supplementary Information and Supplementary Fig. S11). Although the precise molecular mechanism of how AML1 and the Foxp3–AML1 complex control their

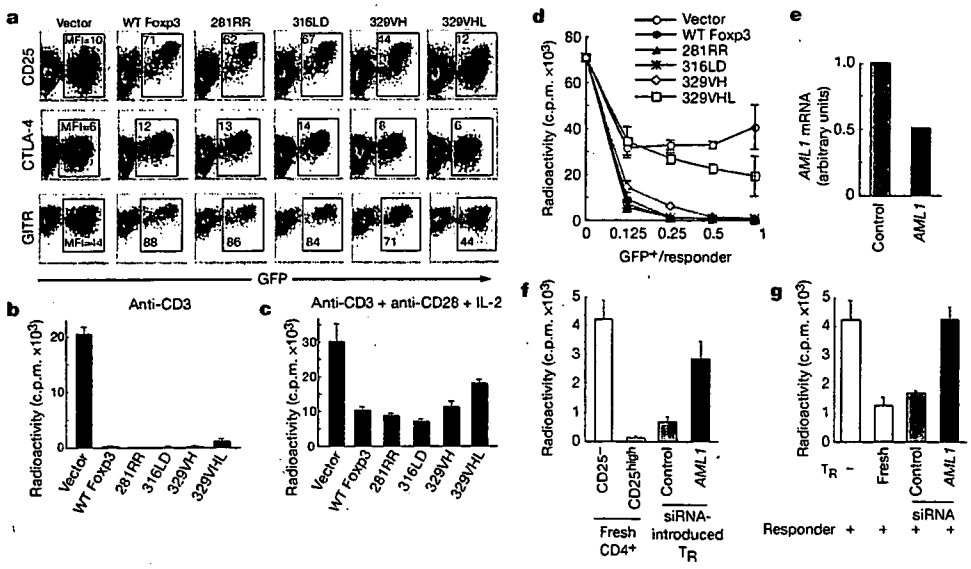

Figure 4 | Foxp3 requires interaction with AML1 to confer T_R-cell phenotype and function on conventional T cells. **a**, Mouse conventional T cells transduced with pMCsIg vector encoding wild-type (WT) or mutant Foxp3 shown in Fig. 3g–j were stained with anti-CD25 (top), anti-CTLA-4 (intracellular, middle) or anti-GITR (bottom), and analysed by flow cytometry. MFI, mean fluorescence intensity. **b**, **c**, Proliferation of sorted GFP^+ cells in the presence of soluble anti-CD3 and antigen-presenting cells (APCs) without (**b**) or with (**c**) IL-2 and anti-CD28, measured by [^{3}H]thymidine incorporation; results are means ± s.d. for triplicate cultures. **d**, Suppressive activity of T cells transduced with wild-type or mutant Foxp3. Graded doses of sorted GFP^+ cells were cultured with freshly prepared $CD25^-CD4^+$ cells for 72 h with soluble anti-CD3 and APCs, and [^{3}H]thymidine incorporation was measured as in **b**. **e**, Knockdown of AML1 results in repression of *AML1* mRNA in human primary $CD25^{high}CD4^+$ T_R cells. Relative expression of AML1 was quantified by real-time polymerase chain reaction, using HPRT as an internal control. **f**, Proliferation of control or *AML1* siRNA (shown in Fig. 1g as AML1 no. 1)-introduced human primary $CD25^{high}CD4^+$ T_R cells in the presence of soluble anti-CD3 and APCs. **g**, Suppressive activity of human primary $CD25^{high}CD4^+$ T_R cells transduced with control or *AML1* siRNA. Fresh or siRNA-transduced $CD25^{high}CD4^+$ T_R cells were mixed with freshly prepared $CD25^-CD4^+$ responder T cells, and stimulated by soluble anti-CD3 in the presence of APCs. Proliferation of cells was assessed by [^{3}H]thymidine incorporation and is shown as mean ± s.d. for triplicate cultures. All experiments were repeated at least three times with similar results.

downstream genes remains to be established, the present study provides several models for transcriptional controls by AML1 and Foxp3 (Supplementary Discussion). In addition, Foxp3 could bind to two other members of the AML/Runx protein family, AML2 (Runx3) and AML3 (Runx2) (Supplementary Discussion and Supplementary Fig. S12). There are recent reports that polymorphisms of AML1 and AML1-binding sites are associated with the susceptibility to several autoimmune diseases in humans[25–28]. Such genetic polymorphisms might affect T_R-cell-mediated maintenance of immunological self-tolerance (Supplementary Discussion). The interaction between AML1 and Foxp3 may be a potential therapeutic target for controlling physiological and pathological immune responses.

METHODS

RNA interference. Human PBMCs were freshly separated from whole blood and purified to $CD4^+$ T cells. Sorted cells were subsequently transfected with the Stealth RNAi duplex oligonucleotides against *AML1* (HSS141472; Invitrogen). Stealth RNAi negative control GC high was used as a control short interfering RNA (siRNA). At 16 h after transfection, 20 U ml^{-1} human recombinant IL-2 (eBiosciences) was added to the culture. At 40 h after transfection, $CD25^{high}CD4^+$ T_R cells (defined as the high 2% fraction of $CD4^+$ T cells) were sorted. At this time point, control and *AML1* siRNA-introduced T_R cells expressed CD25, FOXP3 and CTLA-4 at equivalent levels (Supplementary Fig. S10). $CD25^-CD4^+$ T cells were similarly sorted and used as responders. $CD3^-$ cells were irradiated (25 Gy) and used as APCs. A total of 10,000 $CD25^{high}CD4^+$ T_R cells were mixed with 20,000 APCs with or without 10,000 responder cells. Cells were stimulated with 20 ng ml^{-1} anti-CD3 (HIT3a; BD Pharmingen) for 4 days. [^{3}H]Thymidine incorporation for the last 8 h of cell culture was measured as an indicator of cell proliferation and is expressed as the mean ± s.d. for triplicate cultures.

Retroviral transduction. For co-transduction experiments, cells were first infected with pMCsIg-AML1 and kept for a further 5 h at 32 °C with 5% CO_2 and were subsequently infected with pGCSamIN–Foxp3. Gene transduction into $CD25^-CD4^+$ conventional T cells and $CD25^+CD4^+$ T_R cells was performed by stimulating cells with plate-bound anti-CD3 (10 μg ml^{-1}) and soluble anti-CD28 (1 μg ml^{-1}) with 100 U ml^{-1} mouse recombinant IL-2 for 16 h. Activated T cells were infected by resuspending cells with viral supernatants supplemented with 100 U ml^{-1} IL-2 and 5 μg ml^{-1} Polybrene, followed by centrifugation for 1 h at 3,200 r.p.m. Cells were cultured at 37 °C with 5% CO_2 for a further 24 h and sorted by Moflo (DakoCytomation) for ELISA analyses.

Received 12 December 2006; accepted 9 February 2007.
Published online 21 March 2007.

1. Shevach, E. M. Regulatory T cells in autoimmmunity. *Annu. Rev. Immunol.* 18, 423–449 (2000).
2. Maloy, K. J. & Powrie, F. Regulatory T cells in the control of immune pathology. *Nature Immunol.* 2, 816–822 (2001).
3. Sakaguchi, S. Naturally arising $CD4^+$ regulatory T cells for immunologic self-tolerance and negative control of immune responses. *Annu. Rev. Immunol.* 22, 531–562 (2004).
4. Hori, S., Nomura, T. & Sakaguchi, S. Control of regulatory T cell development by the transcription factor Foxp3. *Science* 299, 1057–1061 (2003).
5. Fontenot, J. D., Gavin, M. A. & Rudensky, A. Y. Foxp3 programs the development and function of $CD4^+$ $CD25^+$ regulatory T cells. *Nature Immunol.* 4, 330–336 (2003).
6. Khattri, R., Cox, T., Yasayko, S. A. & Ramsdell, F. An essential role for Scurfin in $CD4^+$ $CD25^+$ T regulatory cells. *Nature Immunol.* 4, 337–342 (2003).
7. Fontenot, J. D., Rasmussen, J. P., Gavin, M. A. & Rudensky, A. Y. A function for interleukin 2 in Foxp3-expressing regulatory T cells. *Nature Immunol.* 6, 1142–1151 (2005).
8. Okuda, T., van Deursen, J., Hiebert, S. W., Grosveld, G. & Downing, J. R. AML1, the target of multiple chromosomal translocations in human leukemia, is essential for normal fetal liver hematopoiesis. *Cell* 84, 321–330 (1996).
9. Wang, Q. *et al.* Disruption of the *Cbfa2* gene causes necrosis and hemorrhaging in the central nervous system and blocks definitive hematopoiesis. *Proc. Natl Acad. Sci. USA* 93, 3444–3449 (1996).
10. Taniuchi, I. *et al.* Differential requirements for Runx proteins in CD4 repression and epigenetic silencing during T lymphocyte development. *Cell* 111, 621–633 (2002).
11. Komine, O. *et al.* The Runx1 transcription factor inhibits the differentiation of naive $CD4^+$ T cells into the Th2 lineage by repressing *GATA3* expression. *J. Exp. Med.* 198, 51–61 (2003).
12. Jain, J., Loh, C. & Rao, A. Transcriptional regulation of the *IL-2* gene. *Curr. Opin. Immunol.* 7, 333–342 (1995).
13. Rooney, J. W., Sun, Y. L., Glimcher, L. H. & Hoey, T. Novel NFAT sites that mediate activation of the interleukin-2 promoter in response to T-cell receptor stimulation. *Mol. Cell. Biol.* 15, 6299–6310 (1995).
14. Bruniquel, D. & Schwartz, R. H. Selective, stable demethylation of the interleukin-2 gene enhances transcription by an active process. *Nature Immunol.* 4, 235–240 (2003).
15. Novak, T. J., White, P. M. & Rothenberg, E. V. Regulatory anatomy of the murine interleukin-2 gene. *Nucleic Acids Res.* 18, 4523–4533 (1990).
16. Kitabayashi, I., Yokoyama, A., Shimizu, K. & Ohki, M. Interaction and functional cooperation of the leukemia-associated factors AML1 and p300 in myeloid cell differentiation. *EMBO J.* 17, 2994–3004 (1998).
17. Yagi, H. *et al.* Crucial role of FOXP3 in the development and function of human $CD25^+$ $CD4^+$ regulatory T cells. *Int. Immunol.* 16, 1643–1656 (2004).
18. Walker, M. R. *et al.* Induction of FoxP3 and acquisition of T regulatory activity by stimulated human $CD4^+$ $CD25^-$ T cells. *J. Clin. Invest.* 112, 1437–1443 (2003).
19. Fontenot, J. D. *et al.* Regulatory T cell lineage specification by the forkhead transcription factor Foxp3. *Immunity* 22, 329–341 (2005).
20. Ono, M., Shimizu, J., Miyachi, Y. & Sakaguchi, S. Control of autoimmune myocarditis and multiorgan inflammation by glucocorticoid-induced TNF receptor family-related protein^{high}, Foxp3-expressing $CD25^+$ and $CD25^-$ regulatory T cells. *J. Immunol.* 176, 4748–4756 (2006).
21. Kanno, Y., Kanno, T., Sakakura, C., Bae, S. C. & Ito, Y. Cytoplasmic sequestration of the polyomavirus enhancer binding protein 2 (PEBP2)/core binding factor α (CBFα) subunit by the leukemia-related PEBP2/CBFβ-SMMHC fusion protein inhibits PEBP2/CBF-mediated transactivation. *Mol. Cell. Biol.* 18, 4252–4261 (1998).
22. Wu, Y. *et al.* FOXP3 controls regulatory T cell function through cooperation with NFAT. *Cell* 126, 375–387 (2006).
23. Thornton, A. M. & Shevach, E. M. $CD4^+$ $CD25^+$ immunoregulatory T cells suppress polyclonal T cell activation *in vitro* by inhibiting interleukin 2 production. *J. Exp. Med.* 188, 287–296 (1998).
24. Takahashi, T. *et al.* Immunologic self-tolerance maintained by $CD25^+$ $CD4^+$ naturally anergic and suppressive T cells: induction of autoimmune disease by breaking their anergic/suppressive state. *Int. Immunol.* 10, 1969–1980 (1998).
25. Brenner, O. *et al.* Loss of Runx3 function in leukocytes is associated with spontaneously developed colitis and gastric mucosal hyperplasia. *Proc. Natl Acad. Sci. USA* 101, 16016–16021 (2004).
26. Prokunina, L. *et al.* A regulatory polymorphism in *PDCD1* is associated with susceptibility to systemic lupus erythematosus in humans. *Nature Genet.* 32, 666–669 (2002).
27. Helms, C. *et al.* A putative RUNX1 binding site variant between *SLC9A3R1* and *NAT9* is associated with susceptibility to psoriasis. *Nature Genet.* 35, 349–356 (2003).
28. Tokuhiro, S. *et al.* An intronic SNP in a RUNX1 binding site of *SLC22A4*, encoding an organic cation transporter, is associated with rheumatoid arthritis. *Nature Genet.* 35, 341–348 (2003).

Supplementary Information is linked to the online version of the paper at www.nature.com/nature.

Acknowledgements We thank M. Kakino, R. Ishii and M. Yoshida for technical assistance; F. Rawle for valuable comments on the manuscript; T. Kitamura for the pMCsIg retroviral vector; M. Onodera for the pGCSamIN retroviral vector; and F. Macian for the NFAT-CA construct.

Author Information Reprints and permissions information is available at www.nature.com/reprints. The authors declare no competing financial interests. Correspondence and requests for materials should be addressed to S.S. (shimon@frontier.kyoto-u.ac.jp).

Oncogene (2007) 26, 7231–7239

www.nature.com/onc

ORIGINAL ARTICLE

Mutations of the *HIPK2* gene in acute myeloid leukemia and myelodysplastic syndrome impair AML1- and p53-mediated transcription

X-L Li[1], Y Arai[1], H Harada[2], Y Shima[1], H Yoshida[1], S Rokudai[1], Y Aikawa[1], A Kimura[2] and I Kitabayashi[1]

[1]*Molecular Oncology Division, National Cancer Center Research Institute, Chuo-ku, Tokyo, Japan and* [2]*Research Institute for Radiation Biology and Medicine, Hiroshima University, Minami-ku, Hiroshima, Japan*

The AML1 transcription factor complex is the most frequent target of leukemia-associated chromosomal translocations. Homeodomain-interacting protein kinase 2 (HIPK2) is a part of the AML1 complex and activates AML1-mediated transcription. However, chromosomal translocations and mutations of *HIPK2* have not been reported. In the current study, we screened mutations of the *HIPK2* gene in 50 cases of acute myeloid leukemia (AML) and in 80 cases of myelodysplastic syndrome (MDS). Results indicated there were two missense mutations (R868W and N958I) in the speckle-retention signal (SRS) domain of HIPK2. Subcellular localization analyses indicated that the two mutants were largely localized to nuclear regions with conical or ring shapes, and were somewhat diffused in the nucleus, in contrast to the wild type, which were mainly localized in nuclear speckles. The mutations impaired the overlapping localization of AML1 and HIPK2. The mutants showed decreased activities and a dominant-negative function over wild-type protein in AML1- and p53-dependent transcription. These findings suggest that dysfunction of HIPK2 may play a role in the pathogenesis of leukemia.
Oncogene (2007) **26,** 7231–7239; doi:10.1038/sj.onc.1210523; published online 28 May 2007

Keywords: leukemia; HIPK2; mutation; AML1

Introduction

Leukemia is characterized by autonomous proliferation and impaired differentiation of hematopoietic precursor cells, and is considered to be the result of the accumulation of mutations. The mutations associated with the pathogenesis of leukemia include point mutations, gene rearrangements and chromosomal translocations. The *AML1* gene is the frequent target of leukemia-associated chromosome translocations, such as t(8;21)(q22;q22) (AML1-MTG8/ETO) (Miyoshi *et al.*, 1991), t(3;21)(q26;q22) (AML1-EV11/EAP/MDS1) (Nucifora *et al.*, 1993; Mitani *et al.*, 1994), t(16;21)(q24;q22) (AML1-MTG16) (Gamou *et al.*, 1998) and t(12;21)(p13;q22) (TEL-AML1) (Golub *et al.*, 1995; Romana *et al.*, 1995). AML1 protein forms a heterodimer with CBFβ and binds to the specific DNA sequence to regulate the expression of a number of hematopoietic genes (Meyers *et al.*, 1993; Ogawa *et al.*, 1993). Both AML1 and CBFβ are essential for the development of all definitive hematopoiesis lineages (Okuda *et al.*, 1996; Sasaki *et al.*, 1996; Wang *et al.*, 1996a, b; Okada *et al.*, 1998). AML1 forms complexes with PML and HATs, such as p300/CBP and MOZ, leading to the activation of transcription (Kitabayashi *et al.*, 1998, 2001a; Nguyen *et al.*, 2005). The genes encoding components of the AML1 complex are also the targets of leukemia-associated chromosomal translocations, including t(15;17) (q22;q11.2–q12) (PML-RAR α) (de The *et al.*, 1990, 1991; Kakizuka *et al.*, 1991; Kastner *et al.*, 1992), t(8;22)(p11;q13) (MOZ-p300) (Chaffanet *et al.*, 2000; Kitabayashi *et al.*, 2001b), t(11;22)(q23;q13) (E1A-p300) (Ida *et al.*, 1997), t(8;16)(p11;p13) (MOZ-CBP) (Borrow *et al.*, 1996), t(11;16)(q23;p13) (MLL-CBP) (Satake *et al.*, 1997; Sobulo *et al.*, 1997; Taki *et al.*, 1997) and inv(8)(p11q13)(MOZ-TIF2) (Carapeti *et al.*, 1998, 1999). AML1 mutations have been reported in acute myeloid leukemia (AML) and myelodysplastic syndrome (MDS) (Osato *et al.*, 1999; Imai *et al.*, 2000; Preudhomme *et al.*, 2000). Recently, we found that homeodomain-interacting protein kinase-2 (HIPK2) was both involved in AML1 complex, and in the activation of the AML1 complex (Aikawa *et al.*, 2006). However, chromosomal translocations and mutations of *HIPK2* have not been reported previously.

HIPK2, as well as HIPK1 and HIPK3, is a member of a family of serine/threonine nuclear kinases and localizes to nuclear speckles (Kim *et al.*, 1998; Hofmann *et al.*, 2000; Wang *et al.*, 2001; Moller *et al.*, 2003a). Previous studies have shown there is binding of HIPK2 to various target proteins (Choi *et al.*, 1999; Hofmann *et al.*, 2003; Tomasini *et al.*, 2003; Zhang *et al.*, 2003, 2005; Moller *et al.*, 2003b; Rui *et al.*, 2004; Wiggins *et al.*, 2004), with subsequent modulation of the function of these proteins to corepressors or coactivators. HIPK2

Correspondence: Professor I Kitabayashi, Molecular Oncology Division, National Cancer Center Research Institute, 5-1-1 Tsukiji, Chuo-ku, Tokyo 104-0045, Japan.
E-mail: ikitabay@gan2.ncc.go.jp
Received 12 January 2007; revised 5 April 2007; accepted 6 April 2007; published online 28 May 2007

regulates gene transcription (Kim *et al*., 1998; Choi *et al*., 1999) inhibits cell growth (Pierantoni *et al*., 2001) and is involved in apoptosis (D'Orazi *et al*., 2002; Hofmann *et al*., 2002). HIPK2 activates p53 function, thereby promoting apoptosis following ultraviolet (UV) treatment (D'Orazi *et al*., 2002; Hofmann *et al*., 2002).

Human *HIPK2* has been mapped to chromosome 7q32–q34 (Hofmann *et al*., 2000; Wang *et al*., 2001), which is known to be frequently rearranged in AML, MDS, and in other human neoplasias (Mitelman *et al*., 1997). Moreover, HIPK2 expression is reduced in breast and thyroid carcinomas (Kim *et al*., 1999), thus suggesting HIPK2 as a candidate tumor suppressor gene (Kim *et al*., 1999). In the current study, we screened mutations of *HIPK2* in AML and MDS using denaturing high performance liquid chromatography (DHPLC). We found two missense mutations (R868W and N958I) within the speckle-retention signal (SRS) region of HIPK2 that were associated with the subcellular localization. These findings suggest HIPK2 may be involved in the pathogenesis of leukemia.

Results

Mutations of HIPK2 *gene*

In order to search for mutations in all coding exons of the *HIPK2* gene, we performed DHPLC analysis and direct sequence analysis. One missense mutation was detected in MDS, namely R868W in exon 12, and one missense mutation was detected in AML, namely N958I in exon 13 (Figure 1). The leukemic cells with these mutations showed normal karyotypes and no mutations in the *AML1* gene (data not shown). We also detected several single-nucleotide polymorphisms or nonsense mutations polymorphisms, none of which have been reported previously (Table 1).

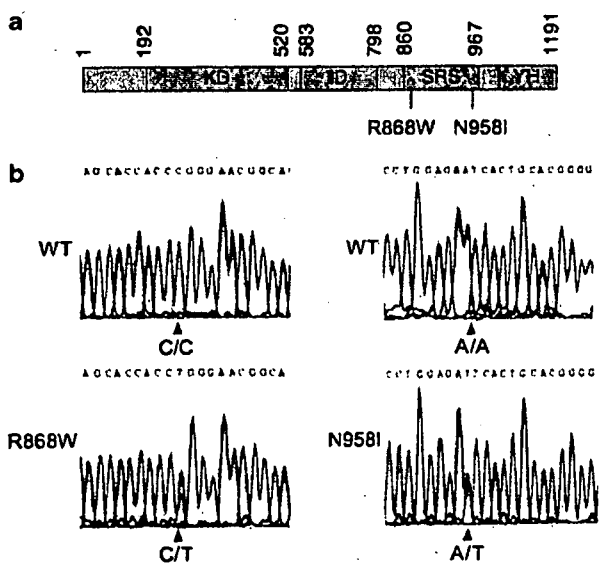

Figure 1 Screening HIPK2 mutations by DHPLC analysis. (a) Schematic representation of the domain structure of HIPK2 showing the location of the mutations identified in this study. KD, kinase domain; ID, interaction domain; SRS, speckle-retention signal; YH, tyrosine and histidine-rich domain. (b) DNA sequencing data of the two missense mutations. C→T was detected in MDS. A→T was detected in AML.

Subcellular localization of the HIPK2 mutants

The two mutations R868W and N958I were located within the SRS region, which is required for localization of HIPK2 in nuclear speckles (Kim *et al*., 1999, 2005; Engelhardt *et al*., 2003). This suggests that the mutations may affect the localization. To investigate subcellular localization, U2OS cells were transfected with wild type, R868W and N958I mutant of HIPK2. Subsequently, we performed immunofluorescence analysis (Figure 2). Wild-type HIPK2 was localized to the small nuclear speckles and these speckles were distributed within the nucleus. However, R868W and N958I mutants exhibited conical or ring shapes, and were diffused in the nucleus.

The HIPK2 mutants fail to colocalize with AML1b

In order to examine whether the HIPK2 mutants are colocalized with AML1b, U2OS cells were

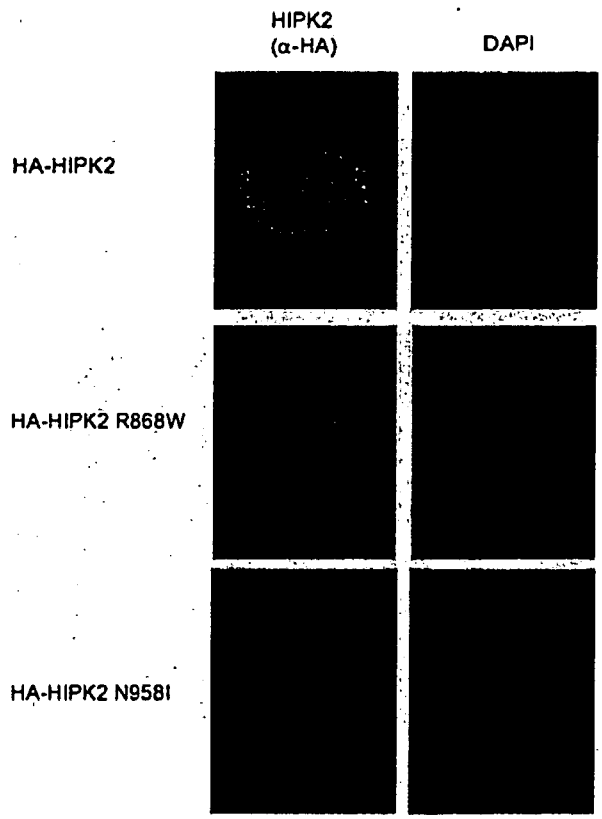

Figure 2 Subcellular localization of HIPK2 proteins (wild type, the mutants R868W and N958I). U2OS cells were transiently transfected with HA-tagged HIPK2 WT, R868W or N958I expression vectors alone. The expressed proteins were detected with anti-HA antibody. DNA was stained with DAPI.

co-transfected with FLAG-tagged AML1b and HA-tagged wild type or mutants of HIPK2 (Figure 3). Without cotransfection of HIPK2, AML1b was diffused in the nucleus. When coexpressed with HIPK2, AML1b was localized to the nuclear dot structures. Moreover, partial overlapping with wild-type HIPK2 was also observed. In contrast, the two mutants of the HIPK2 proteins, R868W and N958I, were not detected overlapping the localization of AML1b.

HIPK2 forms a ternary complex with AML1b and p300, and phosphorylates AML1b and p300 (Aikawa *et al.*, 2006). Therefore, we also investigated whether HIPK2 mutants can interact with and phosphorylate AML1b and p300 (Supplementary Figure 1). No significant differences in interaction or phosphorylation were observed between the wild type and the HIPK2 mutants.

Transcription activation abilities of the HIPK2 mutants

Our data suggest that HIPK2 plays an important role in AML1-mediated and p300-mediated transcription. (Aikawa *et al.*, 2006). To analyse effects of these mutants on transcription activation, reporter experiments were performed. As shown in Figure 4a and b, AML1-mediated and p300-mediated transcription was strongly activated by wild-type HIPK2, but not by the mutants R868W and N958I. These findings suggest that the two HIPK2 mutants lacked transactivation potential.

To determine if the SRS domain is required in order for HIPK2 to stimulate AML1-mediated transcription activation, a series of HIPK2 deletion mutants were constructed and tested for AML1-mediated transactivation. As shown in Figure 5, deletion of the C-terminal region to amino-acid position 1026 did not inhibit but rather stimulated the transactivation. However, further deletion to position 860 completely inhibited the transactivation. These results suggest that the SRS domain is required for HIPK2-mediated transactivation.

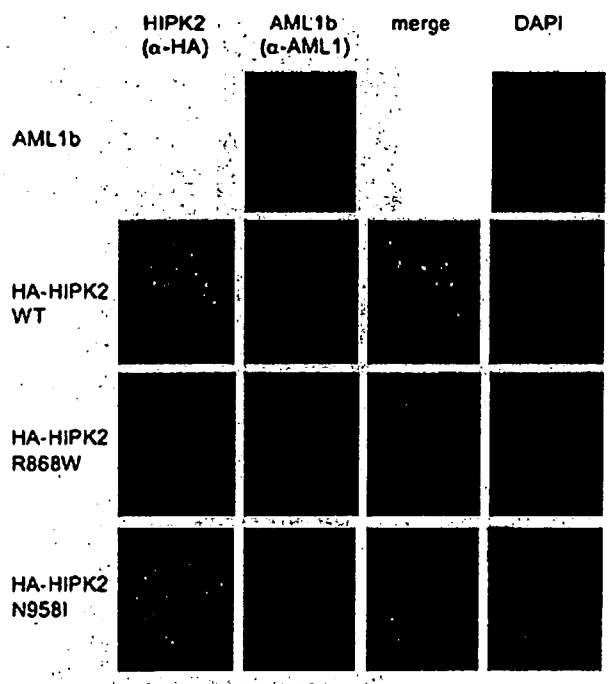

Figure 3 Colocalization of HIPK2 (wild type, the mutants R868W and N958I) with AML1b. U2OS cells were co-transfected with Flag-AML1b and HA-tagged HIPK2 WT, R868W or N958I. Cells were fixed 24 h later and proteins were detected by indirect immunofluorescence staining that used rabbit anti-AML1 and rat anti-HA as primary antibodies. Localization of AML1b is indicated by the red signal, and HIPK2 is indicated by the green signal. Overlapping localization is shown in yellow. DNA was stained with DAPI.

Effect of the HIPK2 mutants on p53 activity

HIPK2 phosphorylates p53 on Ser46, resulting in activation of p53-dependent transcription, cell growth regulation and apoptosis initiation (D'Orazi *et al.*, 2002; Hofmann *et al.*, 2002). To determine whether HIPK2 mutants modulate the transcriptional activity of p53, H1299 cells were co-transfected with the MDM2 promoter and expression vectors encoding p53 and HIPK2 (WT, KD, R868W, N958I). As shown in Figure 6a, p53-dependent transcription was strongly activated by wild-type HIPK2, but not by the mutants R868W and N958I.

To investigate whether HIPK2 affects DNA damage-induced expression of endogenous MDM2, MCF7 cells were transfected with HIPK2 (WT, KD, R868W, N958I) and were exposed to UV. As shown in Figure 6b, expression of MDM2 was increased by wild-type HIPK2, but not by the mutants R868W, N958I and KD. Taken together, these experiments suggest that two HIPK2 mutants affect the p53 pathway.

HIPK2 mutants act as dominant-negative effects in a luciferase assay

In order to investigate whether two HIPK2 mutants exhibit a dominant-negative function, wild-type HIPK2 were co-transfected with the HIPK2 mutants. As shown in Figure 7, the mutants R868W and N958I repressed the wild-type HIPK2-induced activation of both AML1-mediated and p53-mediated transcription in dose-dependent manners. These findings suggest that the two HIPK2 mutants exhibit a dominant-negative function over wild-type HIPK2.

Discussion

Genetic mutations, such as point mutations, gene rearrangement and chromosomal translocations, have been considered to be associated with the pathogenesis of leukemia. The genes encoding AML1 and/or its binding factors are frequent targets of the mutations or chromosome translocations associated with AML and MDS. We have found that HIPK2 is a part of the AML1 complex and is capable of stimulating AML1-mediated transcription activation (Aikawa *et al.*, 2006).

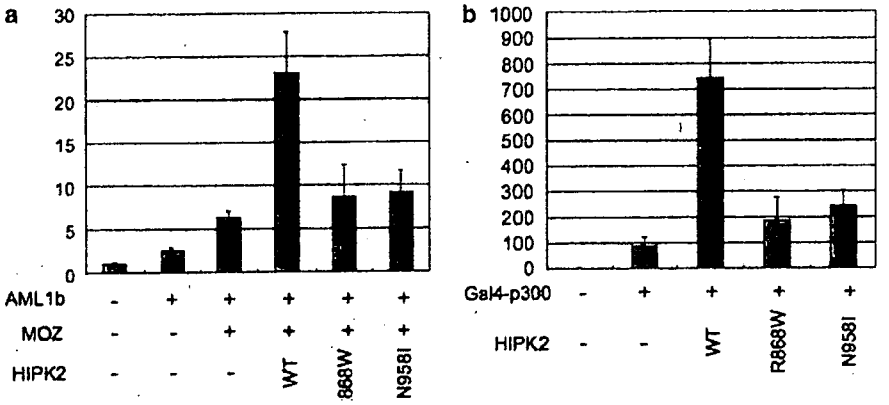

Figure 4 Effects of HIPK2 mutants on AML1-dependent transcription (a) and on transactivation by Gal4-p300 (b). (a) SaOS2 cells were transfected with 50 ng of MPO-luc, 200 ng of LNCX-AML1b, 250 ng of MOZ, 250 ng of wild type or the mutants R868W, N958I of HIPK2 and 2 ng of phRL-CMV. Cell lysates were prepared 24 h after transfection and were analysed for luciferase activity. (b) 293 T cells were transfected with 500 ng of pFR-luc (Gal4-luc), 100 ng of Gal4-p300, 400 ng of wild type or the mutants R868W, N958I of HIPK2 and 2 ng of phRL-CMV. Cell lysates were prepared 24 h after transfection and were analysed for luciferase activity.

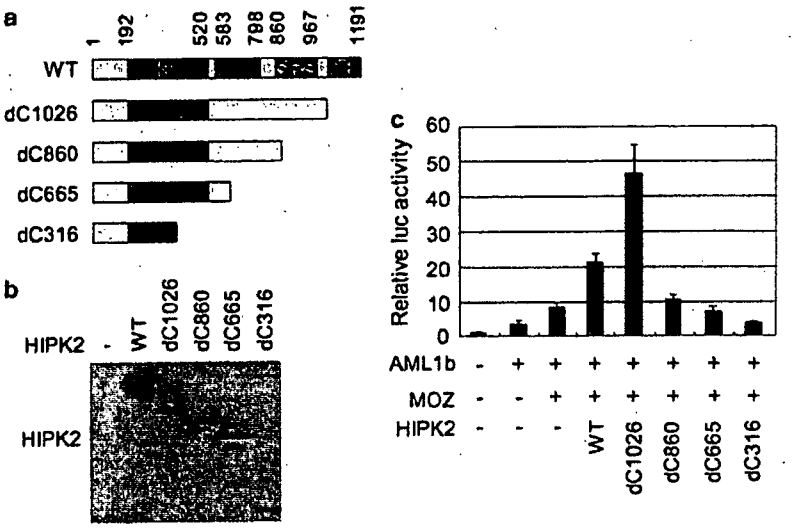

Figure 5 Effects of HIPK2 deletion mutants on AML1-dependent transcription. (a) Structure of HIPK2 deletion mutants. (b) Expression of HIPK2 mutants. 293T cells were transfected with HIPK2 mutants. Cell lysates were prepared 24 h after transfection and were analysed for their expression via immunoblot analysis. (c) Effects of HIPK2 mutants on AML1-mediated transcription activation. SaOS2 cells were transfected with 50 ng of MPO-luc, 200 ng of LNCX-AML1b, 250 ng of MOZ, 250 ng of wild type or deletion mutants of HIPK2 and 2 ng of phRL-CMV. Cell lysates were prepared 24 h after transfection and were analysed for luciferase activity.

These findings suggest that HIPK2 may be also the target of leukemia-associated mutations/chromosome aberrations. However, there have been no previous reports of mutation/chromosome abnormalities in the *HIPK2* gene. In the present study, we examined mutations of the *HIPK2* gene in 50 cases of AML and in 80 cases of MDS. Analyses indicated that there were two missense mutations (R868W and N958I) in the SRS domain of HIPK2. The *HIPK2* gene is mapped to the human chromosome 7q32–q34. Deletion of 7q is frequently found in AML and MDS. Initially, we expected mutation of *HIPK2* to occur in patients with the 7q deletion, thereby resulting in a homozygous loss of functional HIPK2. However, no mutations were found in these types of patients. As a matter of fact, patients with HIPK2 mutations showed normal karyotypes and did not have any other mutations in *AML1*. These results suggest that the mutation of HIPK2 plays a role similar to chromosome translocations and AML1 mutations in the pathogenesis of leukemia. However, further analysis is required to confirm this hypothesis.

Recently, we found that HIPK2 interactions result in the phosphorylation of AML1 and p300 leading to stimulation of AML1-mediated transcription (Aikawa *et al*., 2006). The two missense mutants that we identified here (R868W and N958I) showed decreased activities and a dominant-negative function over wild-type protein in AML1- and p53-dependent

transcription. However, the R868W and N958I mutants affect neither the kinase activity nor interaction with AML1 and p300. The R868W and N958I mutations were found in the SRS domain, in contrast to the kinase domain, for which no mutations were detected. Since SRS is reportedly associated with the HIPK2 localization to nuclear speckles (Kim *et al.*, 1999, 2005; Engelhardt *et al.*, 2003), SRS mutations may affect localization of HIPK2. In fact, R868W and N958I mutations showed impaired localization of HIPK2 in the nuclear speckles. In both wild-type HIPK2 and in AML1, there was colocalization in the nuclear speckles. However, when there were mutations of HIPK2, the overlapping localization was disrupted. Deletion analysis of HIPK2 indicated that the SRS domain is required for HIPK2 to be able to stimulate AML1-mediated transcription activation. These data suggest that the mutations destabilize the localization of HIPK2, leading to dysfunction of the AML1 transcription factor complex.

The mechanism for regulation of the HIPK2 localization to the nuclear speckles via the SRS is poorly understood. Previous studies indicated that HIPK2 is modified by a small ubiquitin-like modifier 1 (SUMO-1) (Kim *et al.*, 1999), and that SUMO modification of HIPK2 occurs at lysine 25 (Hofmann *et al.*, 2005; Sung *et al.*, 2005). The SRS contains a domain that interacts with a SUMO-conjugating (E2) enzyme, mUBC9 (Kim *et al.*, 1999). When there is SUMO modification of HIPK2, this affects localization to the nuclear speckles (Kim *et al.*, 1999, 2005; Engelhardt *et al.*, 2003). It has been reported that SUMO modification regulates localization and activity of target proteins such as RanGAP (Matunis *et al.*, 1996, 1998; Mahajan *et al.*, 1997), PML (Kamitani *et al.*, 1998; Duprez *et al.*, 1999) and CtBP (Lin *et al.*, 2003). However, no differences in SUMO modification were observed between the wild-type and HIPK2 mutants (Supplementary Figure 2). Further biological studies are necessary to clarify how this localization of HIPK2 is regulated by SRS.

We recently found that the *Hipk1*/*Hipk2*-deficient mice exhibit defects in definitive hematopoiesis (Aikawa *et al.*, 2006). We also found that expression levels of HIPK2 increase during granulocyte-colony stimulating factor (G-CSF)-induced differentiation of myeloid cells. These results suggest that HIPK2 plays a role in myeloid cell hematopoiesis and differentiation. Therefore, *HIPK2* mutation may lead to impairment of hematopoiesis and/or differentiation of myeloid cells, resulting in the pathogenesis of leukemia.

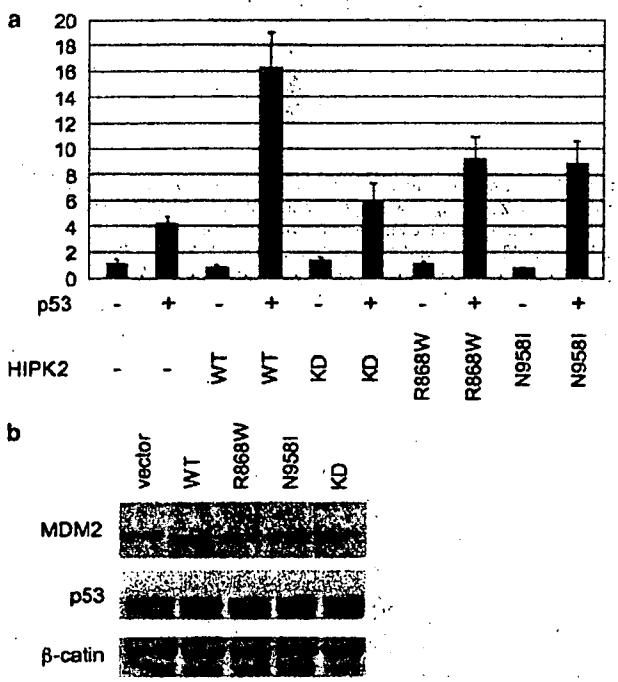

Figure 6 Effects of HIPK2 mutants on p53-dependent transcription. (a) H1299 cells were transfected with 50 ng of MDM2-luc, 2.0 ng of p53, 70 ng of wild type or the mutants (K221A kinase-dead (KD), R868W, N958I) of HIPK2 and 2 ng of phRL-CMV. Cell lysates were prepared 24 h after transfection and were analysed for luciferase activity. (b) MCF7 cells were transfected with wild type or the mutants (R868W, N958I and KD) of HIPK2. The cells were exposed to 30 J/m^2 at 24 h after transfection. After the cells were cultured for 8 h, cell lysates were prepared and analysed by immunoblotting.

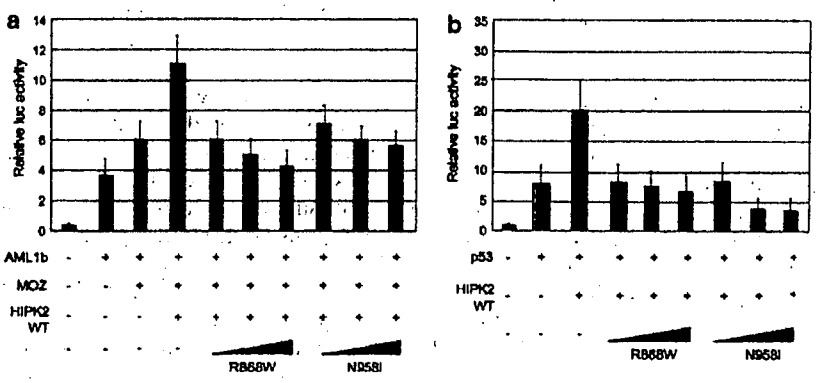

Figure 7 Dominant-negative effects of HIPK2 mutants on wild-type HIPK2 activity. (a) SaOS2 cells were transfected with 50 ng of MPO-luc, 200 ng of LNCX-AML1b, 250 ng of MOZ, 250 ng of wild type, and mutants R868W, N958I of HIPK2. (b) H1299 cells were transfected with 50 ng of MDM2-luc, 2.0 ng of p53, 70 ng of wild type and the mutants R868W, N958I of HIPK2. Cell lysates were prepared 24 h after transfection and were analysed for luciferase activity.

Inactivation of the p53 pathway is associated with cancer development. Although p53 mutations are observed in more than 50% in solid tumors, p53 mutations are found in only 17 and 10% of AML and MDS cases, respectively (Krug *et al.*, 2002), suggesting that leukemia can develop even in the presence of normal p53. In fact, no mutations in p53 were detected in two patients, with *HIPK2* mutations. It has been reported that HIPK2 is involved in induction of p53-dependent transcription, cell cycle and apoptosis (D'Orazi *et al.*, 2002; Hofmann *et al.*, 2002). In this study, we found that HIPK2 mutants exhibited impaired activation of p53-mediated transcription as well as AML1-mediated transcription. Thus, we believe that HIPK2 mutations affect both AML1-mediated cell differentiation and p53-mediated apoptosis to induce leukemia.

In summary, within the SRS, we found two mutations of the *HIPK2* gene, R868W and N958I, which are associated with the subcellular localization of HIPK2. These mutations impaired overlapping localization of AML1 and HIPK2, as well as the activation of AML1-mediated transcription by HIPK2. Furthermore, the two mutants decreased p53-mediated transcriptional activity. Therefore, our results provide new evidence on a possible mechanism for the pathogenesis of leukemia.

Materials and methods

Patient samples

We examined 80 cases of MDS (31 refractory anemia with excess blasts (RAEB), 19 RAEB in transformation (RAEBt), 30 AML following MDS) and 50 cases of AML without antecedent MDS (4 M0, 13 M1, 9 M2, 9 M4, 12 M5, 2 M6, 1 M7) for screening mutations of *HIPK2*. All of these patients were diagnosed by morphology, immunophenotype, karyotype and AML1 mutation analysis as described previously (Harada *et al.*, 2004). Patients with t(15;17), t(8;21), inv(16) or AML1 point mutation were excluded from this analysis. Patient samples were taken after obtaining informed consent and approval from the institutional review board at Hiroshima University.

Screening for HIPK2 *mutations*

Genomic DNA was isolated, and genomic fragments were amplified by PCR using 18 sets of primers (Table 2). The PCR reaction was performed for 35 cycles in a 10 μl mixture containing genomic DNA, 1 μl of 10 × PCR buffer, 0.25 μl of 10 mM dNTP, 2 pmol of each primer and 0.07 U *Taq* polymerase. Each PCR cycle consisted of 94°C for 20 s, 56–60°C for 40 s and 72°C for 1 min, followed by a final extension at 72°C for 10 min. PCR products were electrophoresed in 2% agarose gels. Mutation screening for *HIPK2* was carried out by prescreening with DHPLC analysis (WAVE DNA Fragment Analysis System, Transgenomic, Omaha, NE, USA). If an abnormal peak sample was detected, it was directly sequenced using a Big Dye Terminator Sequencing kit and ABI Prism 3100 Genetic Analyzer.

Cell culture and transfection

SaOS2, 293T, U2OS, MCF7 and H1299 cells were cultured in Dulbecco's modified Eagle's medium or RPMI supplemented with 10% fetal calf serum (FCS) at 37°C and 5% CO_2. U2OS and MCF7 cells were transfected by Effectene (Qiagen, Hilden, Germany) according to the manufacturer's instructions. For the reporter assay, 293T, SaOS2 and H1299 cells were transfected by the calcium phosphate precipitation method.

Plasmids

The human AML1b expression vector pLUCX-FLAG-AML1b, human p300 expression vector pLUCX-FLAG-p300, human MOZ expression pLUCX-FLAG-MOZ, human HIPK2 expression vector pLUCX-HA-HIPK2, pLUCX-HA-HIPK2 KD, human p53 expression vector pLUCX-FLAG-p53, MDM2-luc and MPO-luc have been described previously (Kitabayashi *et al.*, 2001a; Aikawa *et al.*, 2006). The expression vectors of the HIPK2 mutants, LUCX-HA-HIPK2 R868W, LUCX-HA-HIPK2 N958I, were generated by site-specific mutagenesis using overlapping extension PCR. The sequences of these constructs were checked by DNA sequencing.

Table 1 Mutations and SNPs of *the HIPK2* gene in AML and MDS

	Nucleotides		*Amino acids*		*Populations*	
	Positions	*Changes*	*Positions*	*Changes*	*AML*	*MDS*
Missense mutations						
Exon12	2602	C to T	868	R to W		1/80 (1.25%)
Exon13	2873	A to T	958	N to I	1/50 (2%)	
SNPs						
Exon2	891	C to T			8/50 (16%)	19/80 (23.75%)
Exon2	1059	C to G			15/50 (30%)	30/80 (37.5%)
Exon6	1557	C to T			1/50 (2%)	2/80 (2.5%)
Exon10	2145	G to A				1/80 (1.25%)
Exon12	2682	G to T			1/50 (2%)	
Intron3	−56 from exon 4	A to G				2/80 (2.5%)
Intron4	−4 from exon 5	G to A			1/50 (2%)	
Intron10	−9 from exon 11	G to C				1/80 (1.25%)
Intron13	−4 from exon 14	G to A				1/80 (1.25%)

Abbreviations: SNPs, single-nucleotide polymorphisms; *HIPK2*, homeodomain-interacting protein kinase-2; AML, acute myeloid leukemia; MDS, myelodysplastic syndrome.

Table 2 The primer sets for DHPLC for the *HIPK2* gene

Exons	*Forward primers*	*Reverse primers*
Exon2a	GTACCAAGGTGACTCCGATACTT	CAGTGCTTCGACGCATTAGGTTG
Exon2b	CAGCCACCACAACCGTCAG	CGTTTCCAGCACTTGACCACT
Exon2c	CTGTCTCCTTGTGGACGGTCT	ATGTTGGAGCAGAACCTCTATGACT
Exon2d	GTTTGAGGTCAGCGTGGATAA	GCCACTGCCACCACGTCTAC
Exon3	GCTTCCTGCATTTCCAACTTGCT	CAATGAAATGCTAATCCAGGCTA
Exon4	CTCAAAGCCAGCAGAGCCATTAG	TCCCTAAGCGCTGGGCCACT
Exon5	TGGGAAAGAGACCCTCTGTGAGA	CAGAAGTCTTGCTGCCCTTGGTT
Exon6	TCAGGAGGAAGTTACAGGGCAAA	CTTTAAAGTTTGCCGATCCCTGG
Exon7	CATCCCACGTTACCCTCTTCCC	AGTCCTGAGGCTCACACTG
Exon8	CCAACATGCCACCTCCCTCATTT	CAGAGGCCGTTCTGTAAGAAGCA
Exon9	AGCTGTTCACAGCGTCTCAGCTA	TAGGGAGAGAGGGAGTGGAGATA
Exon10	ATCAATTATGTGATTAGCAAACATGGTC	ACGTGCCTCCCATCCCAGAC
Exon11	GGAAGCTTGATCTTATAGAGGAG	CATTTCTTTAGCACTCACATCCC
Exon12	GGGCCTGACCTTCCTCTGTG	CCTCCCGGCTCCTTCCTG
Exon13	CTCACGGCCTTCTCCCACCT	TACAGCAACATTTCTAGCAGCAG
Exon14	GCTGGGACCCTGCCACTGAT	CTCTGAAGCGGAAGGATGAGGG
Exon15a	CTCCTCCCATTCCTTCCTCCC	GTGGGTATCCAGTGTAGACGGTG
Exon15b	CCACCATCCACCCGAGTCAG	GAATGGGTTCTTGAGCTGGGTTT

Abbreviations: DHPLC, denaturing high performance liquid chromatography; *HIPK2*, homeodomain-interacting protein kinase 2.

Immunofluorescence analysis
U2OS cells were grown in four-well chamber slides and co-transfected with various expression vectors. Twenty-four hours after being co-transfected, cells were fixed for 10 min with 4% paraformaldehyde at room temperature, then permeabilized with 0.1% Triton-X 100 in phosphate-buffered saline (PBS) for 10 min. Next, cells were washed three times with PBS and blocked with 0.2% FCS at 4°C for overnight. Cells were incubated with primary antibodies in PBS containing 0.2% FCS for 1 h at room temperature. Cellular nuclei were stained by 4′,6-diamidino-2-phenylindole (DAPI). Images under a fluorescence microscope (Olympus, Melville, NY, USA) were captured with a CoolSNAP-HQ CCD camera (Roper Scientific, Ottobrunn, Germany) at a magnification of ×60.

Luciferase assay
SaOS2, 293T or H1299 cells were co-transfected with various expression vectors in 24-well plates, and luciferase activity was assayed after 24 h using a luminometer Lumat LB9507 (Berthold, Bad Wildbad, Germany) according to the manufacturer's protocol (Promega, Madison, WI, USA). Results of reporter assays represent the average values for relative luciferase activity generated from three independent experiments that were normalized using the activity of the enzyme from phRL-CMV as an internal control.

Immunoprecipitation, immunoblotting and antibodies
For immunoprecipitation experiments, cell were lysed in a lysis buffer containing 250 mM NaCl, 20 mM sodium phosphate pH 7.0, 30 mM sodium pyrophosphate, 10 mM NaF, 0.1% NP-40, 5 mM dithiothreitol, 1 mM phenylmethylsulphonylfluoride and protease inhibitor. Cell lysates were incubated with anti-FLAG antibody-conjugated agarose beads (Sigma, St Louis, MO, USA) and slightly rotated at 4°C overnight. The absorbed beads were washed three times with lysis buffer. Precipitated proteins were eluted from the beads by FLAG peptide and dissolved with the same volume of 2× sodium dodecyl sulfate (SDS) sample buffer. When immunoprecipitation was not performed, total protein lysates were prepared in 2× SDS sample buffer. Antibodies were detected by chemiluminescence using ECL plus Detection Reagents (Amersham Biosciences, Buckinghamshire, UK). The primary antibodies used in this study were anti-FLAG (M2) (Sigma), anti-HA (3F10) (Roche, Basel, Switzerland), anti-human AML rabbit polyclonal, and anti-p300 rabbit polyclonal (N15) antibodies.

References

Aikawa Y, Nguyen LA, Isono K, Takakura N, Tagata Y, Schmitz ML *et al.* (2006). Roles of HIPK1 and HIPK2 in AML1- and p300-dependent transcription, hematopoiesis and blood vessel formation. *EMBO J* **25**: 3955–3965.

Borrow J, Stanton Jr VP, Andresen JM, Becher R, Behm FG, Chaganti RS *et al.* (1996). The translocation t(8;16)(p11;p13) of acute myeloid leukaemia fuses a putative acetyltransferase to the CREB-binding protein. *Nat Genet* **14**: 33–41.

Carapeti M, Aguiar RC, Goldman JM, Cross NC. (1998). A novel fusion between MOZ and the nuclear receptor coactivator TIF2 in acute myeloid leukemia. *Blood* **91**: 3127–3133.

Carapeti M, Aguiar RC, Watmore AE, Goldman JM, Cross NC. (1999). Consistent fusion of MOZ and TIF2 in AML with inv(8)(p11q13). *Cancer Genet Cytogenet* **113**: 70–72.

Chaffanet M, Gressin L, Preudhomme C, Soenen-Cornu V, Birnbaum D, Pebusque MJ. (2000). MOZ is fused to p300 in an acute monocytic leukemia with t(8;22). *Genes Chromosomes Cancer* **28**: 138–144.

Choi CY, Kim YH, Kwon HJ, Kim Y. (1999). The homeodomain protein NK-3 recruits Groucho and a histone deacetylase complex to repress transcription. *J Biol Chem* **274**: 33194–33197.

D'Orazi G, Cecchinelli B, Bruno T, Manni I, Higashimoto Y, Saito S *et al.* (2002). Homeodomain-interacting protein kinase-2 phosphorylates p53 at Ser 46 and mediates apoptosis. *Nat Cell Biol* **4**: 11–19.

de The H, Lavau C, Marchio A, Chomienne C, Degos L, Dejean A. (1991). The PML-RAR alpha fusion mRNA generated by the t(15;17) translocation in acute promyelocytic leukemia encodes a functionally altered RAR. *Cell* **66**: 675–684.

de Thé H, Vivanco-Ruiz MM, Tiollais P, Stunnenberg H, Dejean A. (1990). Identification of a retinoic acid responsive element in the retinoic acid receptor beta gene. *Nature* **343**: 177–180.

Duprez E, Saurin AJ, Desterro JM, Lallemand-Breitenbach V, Howe K, Boddy MN *et al.* (1999). SUMO-1 modification of the acute promyelocytic leukaemia protein PML: implications for nuclear localisation. *J Cell Sci* **112**(Part 3): 381–393.

Engelhardt OG, Boutell C, Orr A, Ullrich E, Haller O, Everett RD. (2003). The homeodomain-interacting kinase PKM (HIPK-2) modifies ND10 through both its kinase domain and a SUMO-1 interaction motif and alters the posttranslational modification of PML. *Exp Cell Res* **283**: 36–50.

Gamou T, Kitamura E, Hosoda F, Shimizu K, Shinohara K, Hayashi Y *et al.* (1998). The partner gene of AML1 in t(16;21) myeloid malignancies is a novel member of the MTG8(ETO) family. *Blood* **91**: 4028–4037.

Golub TR, Barker GF, Bohlander SK, Hiebert SW, Ward DC, Bray-Ward P *et al.* (1995). Fusion of the TEL gene on 12p13 to the AML1 gene on 21q22 in acute lymphoblastic leukemia. *Proc Natl Acad Sci USA* **92**: 4917–4921.

Harada H, Harada Y, Niimi H, Kyo T, Kimura A, Inaba T. (2004). High incidence of somatic mutations in the AML1/RUNX1 gene in myelodysplastic syndrome and low blast percentage myeloid leukemia with myelodysplasia. *Blood* **103**: 2316–2324.

Hofmann TG, Jaffray E, Stollberg N, Hay RT, Will H. (2005). Regulation of homeodomain-interacting protein kinase 2 (HIPK2) effector function through dynamic small ubiquitin-related modifier-1 (SUMO-1) modification. *J Biol Chem* **280**: 29224–29232.

Hofmann TG, Mincheva A, Lichter P, Droge W, Schmitz ML. (2000). Human homeodomain-interacting protein kinase-2 (HIPK2) is a member of the DYRK family of protein kinases and maps to chromosome 7q32-q34. *Biochimie* **82**: 1123–1127.

Hofmann TG, Moller A, Sirma H, Zentgraf H, Taya Y, Droge W *et al.* (2002). Regulation of p53 activity by its interaction with homeodomain-interacting protein kinase-2. *Nat Cell Biol* **4**: 1–10.

Hofmann TG, Stollberg N, Schmitz ML, Will H. (2003). HIPK2 regulates transforming growth factor-beta-induced c-Jun NH(2)-terminal kinase activation and apoptosis in human hepatoma cells. *Cancer Res* **63**: 8271–8277.

Ida K, Kitabayashi I, Taki T, Taniwaki M, Noro K, Yamamoto M *et al.* (1997). Adenoviral E1A-associated protein p300 is involved in acute myeloid leukemia with t(11;22)(q23;q13). *Blood* **90**: 4699–4704.

Imai Y, Kurokawa M, Izutsu K, Hangaishi A, Takeuchi K, Maki K *et al.* (2000). Mutations of the AML1 gene in myelodysplastic syndrome and their functional implications in leukemogenesis. *Blood* **96**: 3154–3160.

Kakizuka A, Miller Jr WH, Umesono K, Warrell Jr RP, Frankel SR, Murty VV *et al.* (1991). Chromosomal translocation t(15;17) in human acute promyelocytic leukemia fuses RAR alpha with a novel putative transcription factor, PML. *Cell* **66**: 663–674.

Kamitani T, Kito K, Nguyen HP, Wada H, Fukuda-Kamitani T, Yeh ET. (1998). Identification of three major sentrinization sites in PML. *J Biol Chem* **273**: 26675–26682.

Kastner P, Perez A, Lutz Y, Rochette-Egly C, Gaub MP, Durand B *et al.* (1992). Structure, localization and transcriptional properties of two classes of retinoic acid receptor alpha fusion proteins in acute promyelocytic leukemia (APL): structural similarities with a new family of oncoproteins. *EMBO J* **11**: 629–642.

Kim YH, Choi CY, Kim Y. (1999). Covalent modification of the homeodomain-interacting protein kinase 2 (HIPK2) by the ubiquitin-like protein SUMO-1. *Proc Natl Acad Sci USA* **96**: 12350–12355.

Kim YH, Choi CY, Lee SJ, Conti MA, Kim Y. (1998). Homeodomain-interacting protein kinases, a novel family of co-repressors for homeodomain transcription factors. *J Biol Chem* **273**: 25875–25879.

Kim YH, Sung KS, Lee SJ, Kim YO, Choi CY, Kim Y. (2005). Desumoylation of homeodomain-interacting protein kinase 2 (HIPK2) through the cytoplasmic-nuclear shuttling of the SUMO-specific protease SENP1. *FEBS Lett* **579**: 6272–6278.

Kitabayashi I, Aikawa Y, Nguyen LA, Yokoyama A, Ohki M. (2001a). Activation of AML1-mediated transcription by MOZ and inhibition by the MOZ-CBP fusion protein. *EMBO J* **20**: 7184–7196.

Kitabayashi I, Aikawa Y, Yokoyama A, Hosoda F, Nagai M, Kakazu N *et al.* (2001b). Fusion of MOZ and p300 histone acetyltransferases in acute monocytic leukemia with a t(8;22)(p11;q13) chromosome translocation. *Leukemia* **15**: 89–94.

Kitabayashi I, Yokoyama A, Shimizu K, Ohki M. (1998). Interaction and functional cooperation of the leukemia-associated factors AML1 and p300 in myeloid cell differentiation. *EMBO J* **17**: 2994–3004.

Krug U, Ganser A, Koeffler HP. (2002). Tumor suppressor genes in normal and malignant hematopoiesis. *Oncogene* **21**: 3475–3495.

Lin X, Sun B, Liang M, Liang YY, Gast A, Hildebrand J *et al.* (2003). Opposed regulation of corepressor CtBP by SUMOylation and PDZ binding. *Mol Cell* **11**: 1389–1396.

Mahajan R, Delphin C, Guan T, Gerace L, Melchior F. (1997). A small ubiquitin-related polypeptide involved in targeting RanGAP1 to nuclear pore complex protein RanBP2. *Cell* **88**: 97–107.

Matunis MJ, Coutavas E, Blobel G. (1996). A novel ubiquitin-like modification modulates the partitioning of the Ran-GTPase-activating protein RanGAP1 between the cytosol and the nuclear pore complex. *J Cell Biol* **135**: 1457–1470.

Matunis MJ, Wu J, Blobel G. (1998). SUMO-1 modification and its role in targeting the Ran GTPase-activating protein, RanGAP1, to the nuclear pore complex. *J Cell Biol* **140**: 499–509.

Meyers S, Downing JR, Hiebert SW. (1993). Identification of AML-1 and the (8;21) translocation protein (AML-1/ETO) as sequence-specific DNA-binding proteins: the runt homology domain is required for DNA binding and protein-protein interactions. *Mol Cell Biol* **13**: 6336–6345.

Mitani K, Ogawa S, Tanaka T, Miyoshi H, Kurokawa M, Mano H *et al.* (1994). Generation of the AML1-EVI-1 fusion gene in the t(3;21)(q26;q22) causes blastic crisis in chronic myelocytic leukemia. *EMBO J* **13**: 504–510.

Mitelman F, Mertens F, Johansson B. (1997). A breakpoint map of recurrent chromosomal rearrangements in human neoplasia. *Nat Genet* **15**: 417–474.

Miyoshi H, Shimizu K, Kozu T, Maseki N, Kaneko Y, Ohki M. (1991). t(8;21) breakpoints on chromosome 21 in acute myeloid leukemia are clustered within a limited region of a single gene, AML1. *Proc Natl Acad Sci USA* **88**: 10431–10434.

Moller A, Sirma H, Hofmann TG, Rueffer S, Klimczak E, Droge W *et al.* (2003a). PML is required for homeodomain-interacting protein kinase 2 (HIPK2)-mediated p53 phos-

phorylation and cell cycle arrest but is dispensable for the formation of HIPK domains. *Cancer Res* 63: 4310–4314.

Moller A, Sirma H, Hofmann TG, Staege H, Gresko E, Ludi KS *et al.* (2003b). Sp100 is important for the stimulatory effect of homeodomain-interacting protein kinase-2 on p53-dependent gene expression. *Oncogene* **22**: 8731–8737.

Nguyen LA, Pandolfi PP, Aikawa Y, Tagata Y, Ohki M, Kitabayashi I. (2005). Physical and functional link of the leukemia-associated factors AML1 and PML. *Blood* **105**: 292–300.

Nucifora G, Begy CR, Erickson P, Drabkin HA, Rowley JD. (1993). The 3;21 translocation in myelodysplasia results in a fusion transcript between the AML1 gene and the gene for EAP, a highly conserved protein associated with the Epstein-Barr virus small RNA EBER 1. *Proc Natl Acad Sci USA* **90**: 7784–7788.

Ogawa E, Maruyama M, Kagoshima H, Inuzuka M, Lu J, Satake M *et al.* (1993). PEBP2/PEA2 represents a family of transcription factors homologous to the products of the Drosophila runt gene and the human AML1 gene. *Proc Natl Acad Sci USA* **90**: 6859–6863.

Okada H, Watanabe T, Niki M, Takano H, Chiba N, Yanai N *et al.* (1998). AML1(−/−) embryos do not express certain hematopoiesis-related gene transcripts including those of the PU.1 gene. *Oncogene* **17**: 2287–2293.

Okuda T, van Deursen J, Hiebert SW, Grosveld G, Downing JR. (1996). AML1, the target of multiple chromosomal translocations in human leukemia, is essential for normal fetal liver hematopoiesis. *Cell* **84**: 321–330.

Osato M, Asou N, Abdalla E, Hoshino K, Yamasaki H, Okubo T *et al.* (1999). Biallelic and heterozygous point mutations in the runt domain of the AML1/PEBP2alphaB gene associated with myeloblastic leukemias. *Blood* **93**: 1817–1824.

Pierantoni GM, Fedele M, Pentimalli F, Benvenuto G, Pero R, Viglietto G *et al.* (2001). High mobility group I (Y) proteins bind HIPK2, a serine-threonine kinase protein which inhibits cell growth. *Oncogene* **20**: 6132–6141.

Preudhomme C, Warot-Loze D, Roumier C, Grardel-Duflos N, Garand R, Lai JL *et al.* (2000). High incidence of biallelic point mutations in the Runt domain of the AML1/PEBP2 alpha B gene in Mo acute myeloid leukemia and in myeloid malignancies with acquired trisomy 21. *Blood* **96**: 2862–2869.

Romana SP, Mauchauffe M, Le Coniat M, Chumakov I, Le Paslier D, Berger R *et al.* (1995). The t(12;21) of acute lymphoblastic leukemia results in a tel-AML1 gene fusion. *Blood* **85**: 3662–3670.

Rui Y, Xu Z, Lin S, Li Q, Rui H, Luo W *et al.* (2004). Axin stimulates p53 functions by activation of HIPK2 kinase through multimeric complex formation. *EMBO J* **23**: 4583–4594.

Sasaki K, Yagi H, Bronson RT, Tominaga K, Matsunashi T, Deguchi K *et al.* (1996). Absence of fetal liver hematopoiesis in mice deficient in transcriptional coactivator core binding factor beta. *Proc Natl Acad Sci USA* **93**: 12359–12363.

Satake N, Ishida Y, Otoh Y, Hinohara S, Kobayashi H, Sakashita A *et al.* (1997). Novel MLL-CBP fusion transcript in therapy-related chronic myelomonocytic leukemia with a t(11;16)(q23;p13) chromosome translocation. *Genes Chromosomes Cancer* **20**: 60–63.

Sobulo OM, Borrow J, Tomek R, Reshmi S, Harden A, Schlegelberger B *et al.* (1997). MLL is fused to CBP, a histone acetyltransferase, in therapy-related acute myeloid leukemia with a t(11;16)(q23;p13.3). *Proc Natl Acad Sci USA* **94**: 8732–8737.

Sung KS, Go YY, Ahn JH, Kim YH, Kim Y, Choi CY. (2005). Differential interactions of the homeodomain-interacting protein kinase 2 (HIPK2) by phosphorylation-dependent sumoylation. *FEBS Lett* **579**: 3001–3008.

Taki T, Sako M, Tsuchida M, Hayashi Y. (1997). The t(11;16)(q23;p13) translocation in myelodysplastic syndrome fuses the MLL gene to the CBP gene. *Blood* **89**: 3945–3950.

Tomasini R, Samir AA, Carrier A, Isnardon D, Cecchinelli B, Soddu S *et al.* (2003). TP53INP1s and homeodomain-interacting protein kinase-2 (HIPK2) are partners in regulating p53 activity. *J Biol Chem* **278**: 37722–37729.

Wang Q, Stacy T, Binder M, Marin-Padilla M, Sharpe AH, Speck NA. (1996a). Disruption of the Cbfa2 gene causes necrosis and hemorrhaging in the central nervous system and blocks definitive hematopoiesis. *Proc Natl Acad Sci USA* **93**: 3444–3449.

Wang Q, Stacy T, Miller JD, Lewis AF, Gu TL, Huang X *et al.* (1996b). The CBFbeta subunit is essential for CBFalpha2 (AML1) function *in vivo*. *Cell* **87**: 697–708.

Wang Y, Hofmann TG, Runkel L, Haaf T, Schaller H, Debatin K *et al.* (2001). Isolation and characterization of cDNAs for the protein kinase HIPK2. *Biochim Biophys Acta* **1518**: 168–172.

Wiggins AK, Wei G, Doxakis E, Wong C, Tang AA, Zang K *et al.* (2004). Interaction of Brn3a and HIPK2 mediates transcriptional repression of sensory neuron survival. *J Cell Biol* **167**: 257–267.

Zhang Q, Nottke A, Goodman RH. (2005). Homeodomain-interacting protein kinase-2 mediates CtBP phosphorylation and degradation in UV-triggered apoptosis. *Proc Natl Acad Sci USA* **102**: 2802–2807.

Zhang Q, Yoshimatsu Y, Hildebrand J, Frisch SM, Goodman RH. (2003). Homeodomain interacting protein kinase 2 promotes apoptosis by downregulating the transcriptional corepressor CtBP. *Cell* **115**: 177–186.

Supplementary Information accompanies the paper on the Oncogene Web site (http://www.nature.com/onc).

MOLECULAR AND CELLULAR BIOLOGY, Aug. 2007, p. 5819–5834 Vol. 27, No. 16
0270-7306/07/$08.00+0 doi:10.1128/MCB.02422-06

PML-Retinoic Acid Receptor α Inhibits PML IV Enhancement of PU.1-Induced C/EBPε Expression in Myeloid Differentiation▽†

Hitoshi Yoshida,[1]* Hitoshi Ichikawa,[2] Yusuke Tagata,[1] Takuo Katsumoto,[1] Kazunori Ohnishi,[3] Yukihiro Akao,[4] Tomoki Naoe,[5] Pier Paolo Pandolfi,[6] and Issay Kitabayashi[1]

Molecular Oncology Division, National Cancer Center Research Institute, Tokyo, Japan[1]; Cancer Transcriptome Project, National Cancer Center Research Institute, Tokyo, Japan[2]; Department of Medicine III, Hamamatsu University School of Medicine, Hamamatsu, Japan[3]; Department of Genetic Diagnosis, Gifu International Institute of Biotechnology, Kakamigahara, Japan[4]; Department of Hematology and Oncology, Nagoya University Graduate School of Medicine, Nagoya, Japan[5]; and Cancer Biology and Genetics Program and Department of Pathology, Memorial Sloan-Kettering Cancer Center, New York, New York[6]

Received 28 December 2006/Returned for modification 23 January 2007/Accepted 17 May 2007

PML and PU.1 play important roles in myeloid differentiation. PML-deficient mice have an impaired capacity for terminal maturation of their myeloid precursor cells. This finding has been explained, at least in part, by the lack of PML action to modulate retinoic acid-differentiating activities. In this study, we found that C/EBPε expression is reduced in PML-deficient mice. We showed that PU.1 directly activates the transcription of the *C/EBPε* gene that is essential for granulocytic differentiation. The type IV isoform of PML interacted with PU.1, promoted its association with p300, and then enhanced PU.1-induced transcription and granulocytic differentiation. In contrast to PML IV, the leukemia-associated PML-retinoic acid receptor α fusion protein dissociated the PU.1/PML IV/p300 complex and inhibited PU.1-induced transcription. These results suggest a novel pathogenic mechanism of the PML-retinoic acid receptor α fusion protein in acute promyelocytic leukemia.

Acute promyelocytic leukemia (APL) has been characterized as a differentiation arrest at the promyelocyte stage due to t(15;17) reciprocal chromosomal translocation that generates a PML-retinoic acid (RA) receptor α (RARA) fusion protein (3, 10). All-*trans* RA (ATRA) induces the differentiation and elimination of APL clones (35). Biochemical evidence that RARA and PML-RARA are bidirectional transactivators (12) and the participation of the *RARA* gene in all APL syndromes examined so far (36) suggest that dominant negative inhibition of RA signaling by PML-RARA plays a critical role in the pathogenesis of APL (25). However, RARA-deficient ($RARA^{-/-}$) mouse models revealed that the retinoid signal is dispensable for myeloid differentiation (11); therefore, how PML-RARA leads to APL requires a revision.

PML contains a characteristic triad of a RING finger, two B boxes (B1 and B2), and a coiled-coil motif, which participates in the formation of high-order multiprotein complexes (20). PML forms discrete "speckle" structures in the nucleus called PML oncogenic domains (PODs) (40). Although the biological functions of PODs remain unclear, they are disrupted by PML-RARA into "microspeckle" structures, which are a hallmark of APL (20). There are several isoforms of PML, which differ in their C termini as a result of alternative splicing (9). Although PML proteins have a number of pleiotropic functions, such as regulation of proliferation, apoptosis, or senescence, at least in vitro (20), little is known about the specific activities of each isoform. PML has been highlighted as a transcriptional coregulator, since it associates with several transcription factors and cofactors (40). Despite the ubiquitous expression of PML proteins and the variety of binding partners, PML-deficient ($PML^{-/-}$) mice do not display significant phenotypes, suggesting that they are not required for but rather modulate normal development. Interestingly, however, the terminal differentiation of granuloid and monocytoid cell lineages is impaired in $PML^{-/-}$ mice (32), but how this occurs remains to be elucidated.

Granulopoiesis is a tightly regulated developmental process that begins with the commitment of myeloid precursors followed by their terminal differentiation, a process that requires cooperative or stepwise actions of lineage-specific transcription factors (6). PU.1 is expressed exclusively in hematopoietic cells (13), and it binds to a purine-rich DNA sequence containing the 5′-GGAA/T-3′ core motif. Although the targeted disruption of the *PU.1* gene can cause multiple hematopoietic aberrations, it invariably causes a defect in the terminal differentiation of myeloid cells (5, 19, 22, 27). PU.1 associates with the p300/CREB-binding protein (CBP) coactivator, at least in vitro (33); however, its essential protein-protein interactions during granulocytic terminal differentiation remain to be explored. PU.1 regulates many myeloid cell-specific genes, including cytokine receptors for granulocyte, granulocyte-macrophage, and macrophage colony-stimulating factor, but the transcriptional cascade that underlies the cell-autonomous effects of PU.1 remains to be elucidated.

CCAAT/enhancer-binding protein ε (C/EBPε) is expressed exclusively in granuloid cells and is essential for the terminal

* Corresponding author. Mailing address: Molecular Oncology Division, National Cancer Center Research Institute, 1-1 Tsukiji 5-Chome, Chuo-Ku, Tokyo 104-0045, Japan. Phone: 81-3-3542-2511, ext. 4752. Fax: 81-3-3542-0688. E-mail: hityoshi@gan2.res.ncc.go.jp.

† Supplemental material for this article may be found at http://mcb.asm.org/.

▽ Published ahead of print on 11 June 2007.

differentiation of committed granulocyte progenitors (17, 34a). C/EBPε is thought to be one critical target of PML-RARA. This is strongly supported by the following observations: (i) C/EBPε is directly regulated by RARA (23); (ii) PML-RARA inhibits the expression of C/EBPε, whereas ATRA restores it (23); (iii) the introduction of C/EBPε into APL cells can mimic the ability of ATRA to drive granulocyte differentiation in vitro and repress the leukemic phenotype of APL in vivo (29); and (iv) APL cells lack secondary granules, which is the prominent characteristic of APL cells and is consistent with a deregulation of C/EBPε expression (7, 34a).

To clarify the role of PML-RARA in the pathogenesis of APL, especially how it causes the arrest of granulocytic differentiation, we focused on the biological properties of PML-RARA and how it perturbs PML function. We show for the first time that the impaired granulopoiesis in *PML*$^{-/-}$ mice is associated with the reduced expression of C/EBPε. In addition, PU.1 directly regulates C/EBPε expression, and PML modulates it by promoting the formation of a PU.1/p300 complex in an isoform-specific manner. Finally, we show that PML-RARA can block granulopoiesis by the direct transrepression of a PU.1/PML/p300 ternary complex and propose a model for how PML-RARA acts as a dominant-negative inhibitor of PML-induced transcription. These results should provide a new insight into how PML-RARA causes leukemia and should help identify new molecular targets for the treatment of APL.

MATERIALS AND METHODS

Mice and cell lines. PML-deficient mice were generated as described previously (32). Mice over 40 weeks of age were analyzed. All animals were maintained under specific-pathogen-free, temperature-controlled conditions throughout this study, in accordance with institutional guidelines. Written approval for all animal experiments was obtained from the local Animal Experiments Committee of the National Cancer Center Research Institute.

Interleukin-3-dependent myeloid L-G myeloblasts (16) and BOSC23, NIH 3T3, and HeLa cells were obtained from the Japanese Cancer Research Bank (Osaka, Japan).

Flow cytometric analysis. Bone marrow (BM) and peripheral blood cells were prepared by lysing erythrocytes in ammonium chloride buffer. In general, one million cells were incubated on ice for 45 min with the appropriate staining reagents according to standard methods. The reagents used in this study were as follows: peridinin chlorophyll protein-cyanin 5.5-conjugated streptavidin, anti-Mac-1–fluorescein isothiocyanate (M1/70-fluorescein isothiocyanate), anti-c-Kit–allophycocyanin (2B8-allophycocyanin), and anti-Gr-1–biotin (RB6-8C5-biotin). All of the reagents were purchased from Pharmingen (La Jolla, CA). Flow cytometry was performed by using a FACSCalibur apparatus (Becton Dickenson), and the results were analyzed using CELLQUEST software (Becton Dickenson).

Expression vectors. Human cDNAs encoding FLAG- or hemagglutinin (HA)-tagged PML isoforms I, II, III, IV, V, and VI were cloned into pLNCX and pLPCX retroviral mammalian expression vectors as described elsewhere previously (21). The cDNAs for PU.1, PML-RARA, PLZF-RARA, RAR, and retinoid X receptor were kindly provided by Francoise Moreau-Gachelin, Akira Kakizuka, Zu Chen, and Pierre Chambon, respectively. The deletion mutants for PU.1 and PML were constructed by PCR-mediated methods (see the supplemental material). The cDNAs for FLAG-tagged PU.1 and its deletion mutants were cloned into the metallothionein promoter-driven expression vector pMT-CB6+. The PML-RARA cDNA was cloned into the pcDNA3.1/His vector (Invitrogen, Carlsbad, CA) for Xpress tagging. HA-tagged PML-RARA cDNA was also cloned into the puromycin-resistant vector pMT-CB6+puro. HA- or FLAG-tagged p300 expression vectors were described previously (21).

Construction of L-G myeloblast clones. L-G cells (1×10^7) were transfected with 10 μg of PvuI-linearized plasmid pMT-CB6+/PU.1 (FLAG tagged) or its deletion derivatives by electroporation (960 μF, 0.35 kV). Stable clones were selected by the treatment of the cells with 1 mg/ml of G418. The expression of PU.1 was induced with 100 μM of $ZnSO_4$ and verified by Western blotting. Retroviruses were prepared from BOSC23 cells transfected with vector pLPCX encoding HA-tagged PML isoforms I to VI or C-terminal deletion mutants of PML IV, and bulk populations were selected by treatment with 0.6 μg/ml of puromycin.

Antibodies. The following antibodies were used in this study: anti-PU.1 (T-21 rabbit polyclonal; Santa Cruz Biotechnology, Santa Cruz, CA), anti-FLAG (M2 mouse monoclonal; Sigma, St. Louis, MO), anti-p300 (NM11 mouse monoclonal; BD Bioscience, San Diego, CA;), anti-HA (3F10 rat monoclonal; Roche Diagnostics, Mannheim, Germany), anti-C/EBPε (C-22 rabbit polyclonal; Santa Cruz Biotechnology), anti-TFIIB (C-18 rabbit polyclonal; Santa Cruz Biotechnology), and anti-PML (PML001 rabbit polyclonal and 1B4 mouse monoclonal [MBL, Nagoya, Japan] and H-238 rabbit polyclonal [Santa Cruz Biotechnology]).

Immunoprecipitation and Western blotting. Detailed procedures for sample preparation, immunoprecipitation, and Western blotting were described elsewhere previously (21).

Immunostaining. Indirect immunofluorescence was performed as previously described (21).

EMSA. An electrophoretic mobility shift assay (EMSA) was performed according to standard procedures (see the supplemental materials for details). For supershift assays, an anti-PU.1 polyclonal antibody (Santa Cruz Biotechnology) was used.

ChIP. Chromatin immunoprecipitation (ChIP) was performed according to the manufacturer's instructions (UBI, Lake Placid, NY) by using the following primers: 5′-CCCATGAGTACCTATATGCTCA-3′ and 5′-CTCAAATCTGGC CTCCGTCACTG-3′ for region 1, 5′-AAGGCTTACATCTCTCCCTCTG-3′ and 5′-CTGTCACCCACTCCTGTGTG-3′ for region 2, and 5′-CACACGATT GTTTAGAGGTAGAAC-3′ and 5′-GAGACTTTAAGAAGCCCGTAATC-3′ for region 3.

Luciferase reporter assay. The *C/EBPε* promoter region was amplified by genomic PCR and cloned into the pGL3-Basic vector (Promega, Madison, WI) as described previously (34). The putative PU.1 binding sites were mutated by site-directed mutagenesis according to standard procedures (see the supplemental material for details). The cells were transfected with the aid of Effectene transfection reagent according to the manufacturer's instructions (QIAGEN, Valencia, CA). After 36 h, luciferase activity was determined using a Dual Luciferase assay system (Promega) according to the manufacturer's instructions. Values were normalized by the luciferase activity of a cotransfected *Renilla* luciferase-expressing vector (pRL-CMV).

RT-PCR. RNA was isolated according to standard protocols and reverse transcribed with random primer using Superscript II (Invitrogen) according to the manufacturer's instructions. For quantitative reverse transcription (RT)-PCR, the following sets of primers and internal fluorescence probes were purchased from Roche Diagnostics (Indianapolis, IN); mouse *C/EBPε* (catalog no. 04688970001), mouse *GAPDH* (catalog no. 04689089001), and mouse *PML* (catalog no. 04688996001). PCRs were performed using an ABI PRISM 7500 Fast Real-Time RCR system (Perkin-Elmer, Foster City, CA) using TaqMan Universal PCR Master Mix containing specific primers (1.2 μM) and a specific probe (0.1 μM). For conventional RT-PCR, the following sets of primers were used: 5′-GACTACAAAGACGATGACGAC-3′ (forward) and 5′-CAGTAATGGTC GCTATGGCTC-3′ (reverse) for FLAG-tagged human *PU.1* and 5′-CTTCACC ACCATGGAGAAGG-3′ (forward) and 5′-GGCATGGACTGTGGTCATGA G-3′ (reverse) for *GAPDH*.

RESULTS

Impaired granulopoiesis and reduced C/EBPε expression in PML-deficient mice. Flow cytometry analysis of sex-matched littermates revealed that circulating Gr-1^{hi} Mac-1^{+} mature granulocytes were reduced in peripheral blood from *PML*$^{-/-}$ mice (Fig. 1A), as previously described (32). On the other hand, the increase of immature granulocytes in the BM of *PML*$^{-/-}$ mice was demonstrated by a fourfold increase in Gr-1^{+} c-Kit^{+} cells (Fig. 1B). These results suggest that the terminal maturation of granulocytes is impaired in *PML*$^{-/-}$ mice. To investigate the role of PML in normal granulopoiesis, we examined the expression levels of several transcription factors that are supposed to be essential for the process. Western blotting analysis of BM mononuclear cells revealed that PML expression was reduced in proportion to the *PML* genotype.

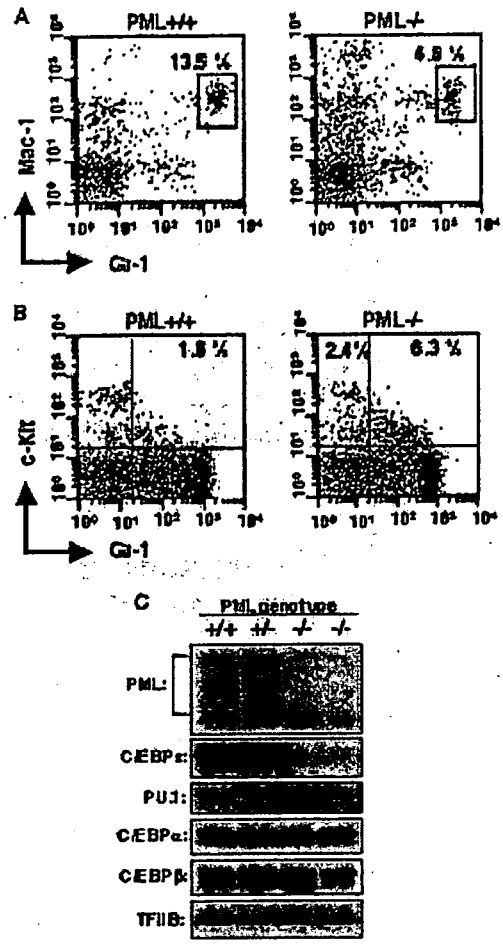

FIG. 1. Impaired granulopoiesis in *PML*$^{-/-}$ mice. (A) Mature granulocytes were reduced in peripheral blood of *PML*$^{-/-}$ mice. Whole peripheral blood cells were stained with anti-Mac-1 and anti-Gr-1 and then analyzed by flow cytometry. (B) Immature granulocytes were increased in BM of *PML*$^{-/-}$ mice. BM cells were stained with anti-Gr-1 and -c-Kit. (C) Reduced expression of C/EBPε in BM mononuclear cells from *PML*$^{-/-}$ mice. Total cell lysates were analyzed by Western blotting.

There was no significant difference in PU.1 and C/EBPα, but C/EBPβ expression was modestly reduced in *PML*$^{-/-}$ mice. On the other hand, C/EBPε expression was reduced in proportion to that of PML (Fig. 1C). These results suggest that the specific involvement of PML in C/EBPε expression may account for its underlying role in granulocytic differentiation.

***C/EBPε* is a direct transcriptional target of PU.1.** To investigate how PML is involved in C/EBPε expression, we first analyzed its promoter. The transcription of the *C/EBPε* gene is regulated mainly by the downstream Pβ promoter, which is highly conserved among different species (2, 34). The DNA sequence around the Pβ promoter is highly rich in purine tracts, which are peculiar features of myeloid cell-specific genes and often serve as potential binding sites for *ets* family transcription factors. These facts prompted us to examine if PU.1 regulates the expression of *C/EBPε*. ChIP assays of HL-60 cells revealed that PU.1 binds to the region 2, which includes the Pβ promoter, in vivo (Fig. 2A). However, we could not detect any significant binding of PU.1 to other genomic regions 4 kb upstream or downstream of the Pβ promoter (regions 1 and 3, respectively). These results indicate that PU.1 binds to a specific genomic region that includes the Pβ promoter. The specificity of this ChIP assay was further confirmed, as the same anti-PU.1 antibody failed to precipitate region 2 in MOLT-4 cells that lack endogenous PU.1 expression (see Fig. S1A in the supplemental material). EMSA detected at least two PU.1 binding regions: region A, between bp −80 and −44, and region B, between bp −40 and −18. PU.1 bound to region A more efficiently than region B (Fig. 2D, left). Inspection of the DNA sequence identified six putative *ets* core motifs (A1 to A3 and B1 to B3) (Fig. 2C). To identify the PU.1 binding sites, we constructed a *C/EBPε* promoter-containing luciferase reporter, introduced either several block mutations or various combinations of site-directed mutations into these motifs, and performed transactivation assays using NIH 3T3 cells (Fig. 2E). As we expected, the response to PU.1 was limited to a region between bp −80 and −18, which contains a purine-rich tract. Luciferase assays further revealed that the response to PU.1 was mediated between positions bp −62 and −57 (A2) and between bp −34 and −29 (B1) (Fig. 2E). Similar results were also obtained for HeLa cells (see Fig. S1B in the supplemental material), suggesting that these effects do not depend on the cell context. Competitive EMSA combined with supershift assays indicated that PU.1 specifically binds to these sites in vitro (Fig. 2D, middle and right panels). Taken together, these results show that PU.1 transactivates the *C/EBPε* gene directly.

PML IV associates with PU.1 in vivo. To investigate the interaction of endogenous PML and PU.1, an immunoprecipitation assay was performed using HL-60 cells. An anti-PML antibody raised against its N terminus successfully immunoprecipitated multiple PML isoforms (Fig. 3A) from HL-60 cell extracts and also pulled down PU.1 together with them (Fig. 3B, left). Reciprocal experiments using an anti-PU.1 antibody revealed the predominant coimmunoprecipitation of a specific PML isoform with a molecular mass of ~75 kDa (Fig. 3B, right). These results indicate the association of these endogenous proteins in myeloid lineage cells. To determine the isoform specificity for PU.1 binding, PU.1 and one of each of the PML isoforms were transiently coexpressed and subjected to immunoprecipitation. PML II and IV specifically interacted with PU.1 (Fig. 3C). An association between PU.1 and the other isoforms, including PML VI, was not successfully detected.

To further confirm those results, we next examined whether these two proteins are colocalized in cells (Fig. 3D). Immunofluorescence revealed that PU.1 was spread throughout the nucleus in NIH 3T3 cells. Upon cotransfection with PML IV, however, PU.1 formed discrete speckles and colocalized prominently with PML IV PODs. Surprisingly, and in contrast with the immunoprecipitation results, PU.1 was not recruited to PML II PODs but instead was recruited to PML VI PODs. Colocalization of PU.1 with both PML IV and VI was also observed in HeLa cells (data not shown). We further examined the subcellular localization of both proteins in mouse embryonic fibroblasts from *PML*$^{-/-}$ mice. Here, we found that PU.1 was also recruited to PML IV PODs but not to PML VI PODs

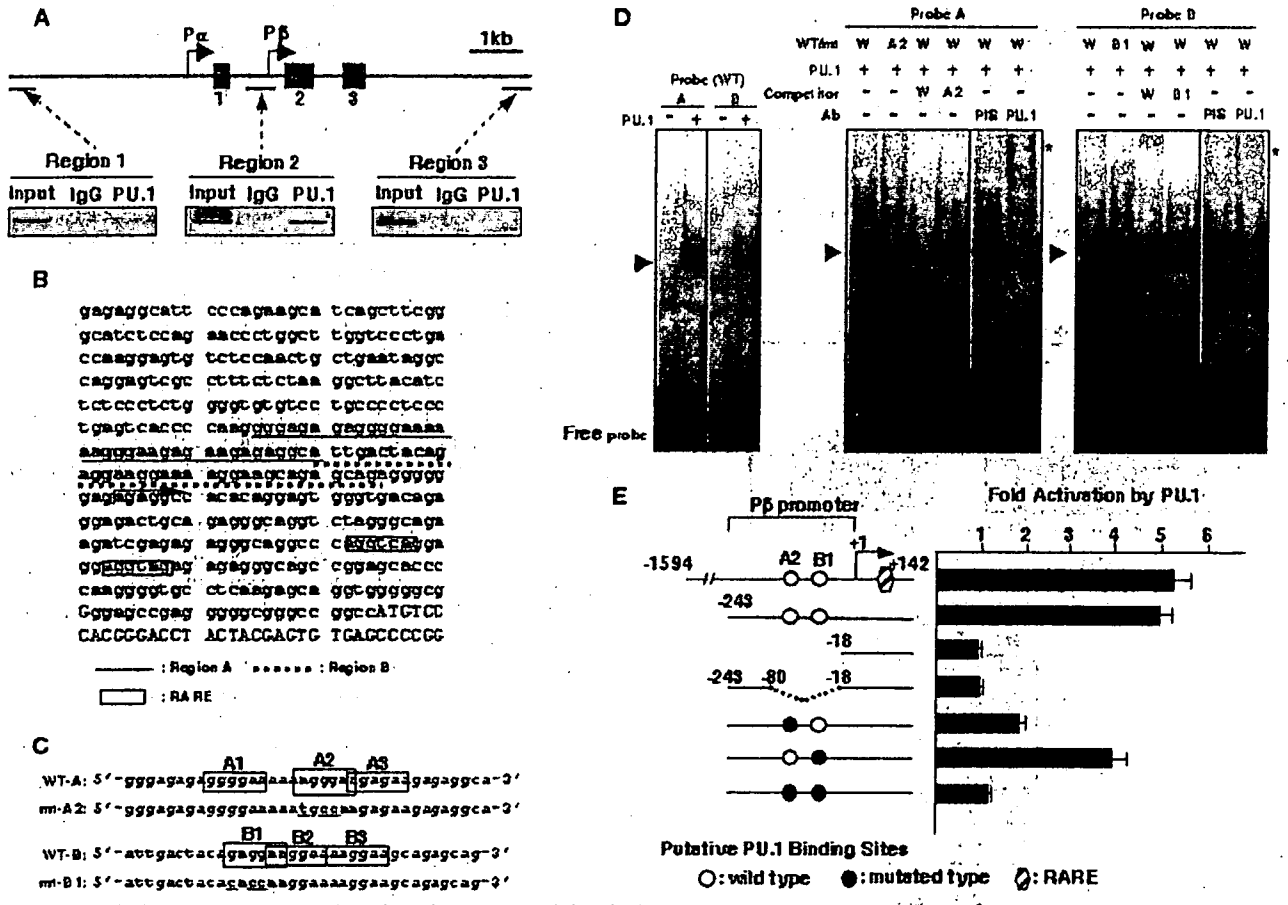

FIG. 2. PU.1 regulates the expression of the *C/EBPε* gene. (A) A ChIP assay shows that PU.1 binds to the promoter region of the *C/EBPε* gene in HL-60 hematopoietic cells. In the schematic of the *C/EBPε* locus, exons are represented by boxes on the line, and transcription start sites are represented by arrows. Three regions examined for PU.1 binding are indicated. Cross-linked HL-60 chromatin was immunoprecipitated with anti-PU.1 antibody (PU.1) or isotype-matched immunoglobulin G (IgG) as a negative control. Three percent of input DNA was also PCR amplified. (B) DNA sequences of the *C/EBPε* promoter region. A major transcriptional start site is indicated by an arrow. The oligonucleotide sequences used for EMSA probes are underlined, and the putative PU.1 binding sites are shown in boldface type. The RARE is shown in boxes. (C) Sequences of wild-type (WT) and mutated (mt) probes used for EMSA. The six putative core PU.1 binding motifs are shown in boxes, and the two PU.1 binding sites tested by EMSA are shown in boldface type. The mutated nucleotides are underlined. (D) Identification of PU.1 in DNA-protein complexes by EMSA using nuclear extracts from BOSC23 cells transfected with the PU.1 expression vector. Arrowheads indicate the PU.1-DNA complexes. Supershifted bands are indicated by asterisks. PIS, rabbit preimmune serum. (E) PU.1 response elements within the *C/EBPε* promoter were confirmed by luciferase reporter assays. A major transcriptional start site is shown as "+1." NIH 3T3 cells were transfected with 0.1 μg of wild-type reporter plasmids containing the region between bp −1594 and +142 or bp −243 and +142 or its mutant derivatives along with 0.1 μg of a PU.1 expression vector. The results are represented as activity (*n*-fold) compared to that of PU.1 and are the average of at least three independent experiments. The error bars represent the standard deviations.

(see Fig. S2 in the supplemental material). These results suggest that the in vivo association between PU.1 and PML IV is of primary importance and that PML VI might indirectly associate with PU.1, although underlying mechanisms remain to be elucidated.

PML IV specifically cooperates with PU.1 to induce terminal differentiation of L-G myeloblasts. We next investigated the ability of each PML isoform to cooperate with PU.1 in the terminal differentiation of L-G myeloid progenitor cells (16). L-G cells were transfected with a vector for expressing PU.1 under the control of a metallothionein promoter (pMT-PU.1). We established several stable clones and confirmed that they morphologically differentiated toward polymorphonuclear cells (PMNs) upon the induction of PU.1 with $ZnSO_4$. To investigate the isoform-specific cooperation between PU.1 and PML, we used a retrovirus to transduce the L-G/MT-PU.1 cells with PML I, II, III, IV, V, VI, or mock (L-G/MT-PU.1/PML isoforms) (Fig. 4A). The level of PU.1 expression following induction with $ZnSO_4$ was the same in all seven cotransfected cells and the parent L-G/MT-PU.1 cells (see Fig. S3A in the supplemental material) (data not shown). Although the expression level of transduced PML IV seemed to be high compared to that of the endogenous one, it was almost comparable to the level of total PML expression (see Fig. S3C in the supplemental material). The induction of PU.1 expression alone retarded cell growth, and the coexpression of PML IV enhanced this effect (Fig. 4B). PU.1 and PML IV also had a synergistic effect on morphological differentiation (Fig. 4C).